Alma Mater Studiorum – Università di Bologna

DOTTORATO DI RICERCA IN

SCIENZE CHIRURGICHE

Ciclo XXVIII

Settore Concorsuale di afferenza: **06/F4**

Settore Scientifico disciplinare: **MED/33**

VASCULARIZED HOMOLOGOUS BONE GRAFT AND BONE MARROW NUCLEATED CELLS TRANSPLANTATION TO ENHANCE ANGIOGENESIS IN THE REPAIR OF CRITICAL SIZE BONE DEFECT: AN ANIMAL STUDY

Presentata da: **Dr. Marco Cavallo**

Coordinatore Dottorato   Relatore

 Prof. Mauro Gargiulo   **Prof. Maurilio Marcacci**

Esame finale anno 2016

INDEX

INTRODUCTION

Repair of a critical size bone defect still represents an issue in orthopedic surgery. Large segmental bone loss usually occurs after traumas or after bone tumor excisions. In such cases, the regeneration for new bone is impaired and surgery is crucial in order to fill the defect. Many different methods have been described up to now, all of them with positive aspects and drawbacks that strongly limit their routine use. The main issue is to fill the bony gap with a vital and integrated bone or bone like material, in order to overcome all the complications that these massive procedures carry with them such as infections, non healing, and multiple revision surgeries.

Bone healing is a complex and articulated process of reconstruction of the bone tissue [1]. The vast majority of bone defects can heal spontaneously under suitable physiological environmental conditions due to the reparative ability of bone. However, new bone generation usually takes place slowly because of decreased blood supply to the fracture site and insufficiency of calcium and phosphorus to strengthen and harden new bone. In addition, large defects, also known as critical bone defects, may not heal spontaneously and can lead to nonunion due to the size of defects or unstable biomechanical properties, hostile wound environment, non optimal surgical procedure or execution, dismetabolic factors, hormones, nutrition, and stress forces [2,3].

CHAPTER 1
LONG BONE DEFECTS

1.1 CRITICAL SIZE DEFECT

A segmental bone defect is labeled in experimental models as "critical" when its length is superior to the healing capabilities of that bone, by definition "the smallest size intraosseous wound in a particular bone and species of animal that will not heal spontaneously during the lifetime of the animal" [4]. Every bone has a different critical value, which differs according to several factors including soft tissue coverage, periosteal presence, age, specie, vascularization, mechanical load, fixation and so on. In animal models every bone in every different specie shows different values, which are mandatory to be kept into consideration when setting up a preclinical study in vivo. In fact, it is mandatory to create in experimental environment a defect which cannot spontaneously heal [5]. Usually for simplicity a critical size defect is considered a gap of a length exceeding 2-2.5 times the diameter of the affected bone [6].

Small size defects can be easily managed with different surgical options, usually by homologous non-vascularized cancellous bone grafting harvested from the iliac crest.

In presence of a "critical size defect" in humans several surgical procedures have been developed over time, all of them with positive aspects and multiple drawbacks, with the result that unfortunately an optimal and safe procedure to treat these occurrences has not yet been developed.

1.2 BONE RESTORATION PROCEDURES

Surgical options available for managing large defects are multiple, the most performed all over the world are bone substitutes, bone transport, non-vascularized grafts, allografts and autologous vascularized fibula pro tibia bone graft.

Bone substitutes or synthetic graft biomaterials are commonly used, leading to a recent develop of a wide range of different substitutes biomaterials commercially available, made of naturally derived tissues, synthetic materials or metals (like the recently released trabecular titanium) [7-11].

The ideal bone graft substitutes should be biocompatible, bioreabsorbable, osteoconductive, osteoinductive, structurally similar to native bone, easy to handle and ready to use. The bone substitutes have many positive aspects: they are virtually unlimited, so the amount of gap to be filled is never an issue, they can be shaped and contoured anatomically according to the specific necessities, and many of them proved to be able to be tolerated by the host cells. The stronger limitation is that the osteointegration is never complete, leading to a non viable material present in a skeletal segment: this highly increases the possibilities of infection, especially in immunocompromised patients (like many of the oncologic resected patients are).

Autograft transplantation is the gold standard, as they encomprises all the three fundamental features for the bone regeneration: osteoinduction, osteoconduction and osteogenesis. Unfortunately, autografts cannot be used for massive bone loss (usually within 5 cms), as their use affects the donor site. The use of these graft, however, is associated with considerable negative side effects. Graft harvest leads to prolonged anesthetic periods and requires personnel. Sometime only an insufficient amounts of graft can be obtained, because the donor sites are limited. This technique commonly carries also the problem of donor site morbidity and the risk of infection [12]. Graft failures usually result from incomplete transplant integration, particularly in large

defects [12]. In addition, graft devitalization due to insufficient graft vascularisation and subsequent resorption processes can lead to decreased mechanical stability.

Autologous vascularized bone grafting is currently one of the procedure of choice because of high osteogenic potential and resistance against reabsorption. The transplantation of vascularised autografts is time consuming and technically demanding: along with the extremely limited availability of donor sites, there is a huge difficulty in the surgical procedure which requires an highly skilled team, the necessity of microvascular techniques for vessels anastomosis [13]. The main advantage is that the bone can be transferred together with soft tissue to cover local soft tissue defect, leading to a higher rate of integration even in long bones with few soft tissue coverage (like tibia: in fact, the most executed procedure is autologous fibula pro tibia graft).

Bone transport is another option for the management of very large bone defects: this technique has been introduced to avoid graft integration-related difficulties, and it is known as the "Ilizarov technique". It is performed with an osteotomy of bone combined with distraction to stimulate bone formation. This procedure has been applied successfully to treat large bone defects, infected non-unions, and limb length discrepancy [14]. However, Ilizarov technique is difficult accepted by the patients because of the massive hardware, the necessary compliance of the long lasting post op protocol, frequent clinical and radiological follow ups, and recurrent pin track infections. The procedure has a very high overall complication rate, but it is still one of the mostly performed procedures in diaphyseal loss in long bones of lower limbs.

1.3 ALLOGRAFT

In the last decade this allograft technique has been widely used for several orthopaedics diseases: in the US more than 5 million bone tissue allografts have been transplanted in the last 10 yrs [15], especially to replace bone and joints lost after metallic implants removal and bone tumors excision [16-18]. Tissue banks use a different technique in bone allograft excision and preparation, and the debate on what should be the better protocol is still ongoing. Donors should undergo a full screening histories (from medical records or relative interviews) and physicals examination, along with a screening laboratory tests for transmissible diseases. Usually the grafts are explanted from the donor with aseptic technique, in a sterile operating room environment after the donor has been washed properly and the skin covered with antiseptic solution. This is usually performed as soon as possible after death of the donor, with general limits of 24 hours if the body has been refrigerated or 12 hours if it has not been refrigerated. In some cases the procurement would be performed immediately after the harvesting of visceral organs. The donor's body is draped in a similar fashion to that used during surgery. Cultures are obtained usually twice on each harvested tissue. Various solutions, such as antibiotics, surfactants, and alcohols, may be used to prepare the allograft tissue. The method of secondary sterilization, also known as terminal sterilization, is used in the cases in which the allografts are not obtained in an aseptic technique [19].

Bone allografting offers the advantage of allowing the surgeon to place a graft of the same anatomic location, with good mechanical and osteoconductive properties. Furthermore, this grafts still contain osteoinductive factors, which give the advantage of a boost to osteoinduction properties. Regarding immunogenicity, bone and tissue allograft tissues can theoretically elicit immune responses in the hosts, mediated via class I and II major histocompatibility complex (MHC) antigens. However, because cell death occurs with tissue processing, the magnitude of immune reaction is really low,

sometimes showing itself as graft reabsorption over time and usually not with the commonly observed rejection processes with soft tissues or organs [6,20-23].

Although autografts are the current gold standard treatment for bone defect regeneration [12], it still has the main disadvantages in the limitation in donor supply [24].

1.4 INNOVATIVE PERSPECTIVE

In order to overcome the major drawbacks of the aforementioned options, the idea to blend bone graft substitutes and the concept of tissue engineering is gaining more and more interest. Several studies in literature reported the ability of bone marrow stem cells (BMSCs) to promote neoangiogenesis. Neo-vascularization is the crucial point in order to provide a regenerative potential to an implanted graft, and for these purpose mesenchymal stem cells are needed. A recently developed technique, arthroscopic bone marrow stem cells (BMSCs) transplantation ("one-step" Technique), involves the harvesting of bone marrow from posterior iliac crest, its concentration directly in operating room, thus without the need of cells' expansion, and the successive transplantation of the cells onto a scaffold in the affected area [25-27].

The use of concentrated bone marrow derived cells has been gaining successful results since it is possible to transplant not only mesenchymal stem cells but also accessory cells that support stem cells' proliferation and differentiation by producing several growth factors. The capability of bone marrow-derived cells to differentiate into both chondral and osseous lineages, thus supporting the hypothesis that in vivo bone marrow-derived cells may be able to fill both chondral and osseus defects associated with the release of trophic molecules, has already been demonstrated [28-33].

CHAPTER 2

ANGIOGENESIS AND OSTEOGENESIS

2.1 THE ROLE OF ANGIOGENESIS IN BONE FORMATION AND FRACTURE HEALING

Osseous tissue is the major structural and supportive connective tissue of the body. Bone is composed of a matrix containing abundant collagen fibers which impart strength, some flex, and resistance to twisting or torsional forces, and of a cement-like ground substance called hydroxyapatite, a mineral complex of calcium phosphate salts makes bone highly resistant to compression forces.

There are two main kinds of bone: trabecular bone, also known as spongy or cancellus bone, and cortical bone also called compact or hard bone. The first gives supporting strength to the end of weight-bearing bone, while cortical bone is on the outside and forms the shaft of the long bones [34]. Cortical bone is dense and solid and surrounds the marrow space, whereas trabecular bone is composed of a honeycomb-like network of trabecular plates and rods interspersed in the bone marrow compartment. Both bone types are composed of osteons. Osteon, also named haversian system, is the fundamental functional unit of bone [34]. The adult human skeleton is composed of 80% cortical bone and 20% trabecular bone overall. Ratios of cortical to trabecular bone are different depending on skeleton sites or bone types [35].

Cortical bone has an outer periosteal surface (periosteum) and inner endosteal surface (endosteum). Both p and periosteum and endosteum are important for appositional growth and fracture repair (Fig. 1a).

15

Despite its inert appearance, bone is a highly dynamic organ continuously resorbed and neoformed. It is a mineralized connective tissue that exhibits four types of cells: osteocytes, osteoblasts, osteogenic cells and osteoclasts. Osteoclasts are large multinuclear cells associated with the resorption of bone, osteoblasts are mononucleate cells from which bone develops, while osteocytes are a mature bone cell type involved in the maintenance of bone tissue and act as mechanosensors. Osteogenic cells are the osteoblast precursors and play an important role in osteogenesis during development and growth and in bone fracture repair in adulthood (Fig. 1b).
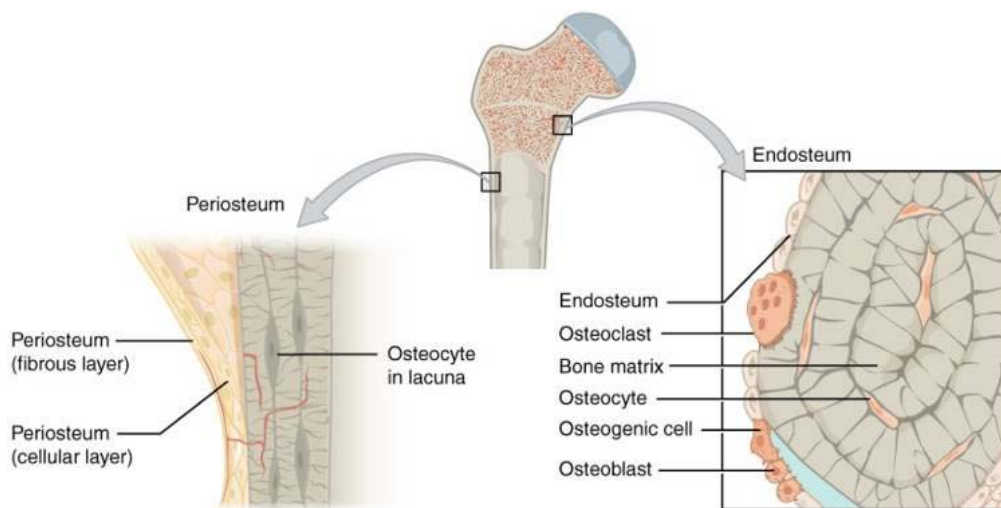

Figure 1 a Bone structure and bone cell types.

Long bones contain two distinct morphological types of layers. Periosteum is a layer of vascular, innervated, dense connective tissue surrounding the non-articular surfaces of bone. The endosteum is a thin layer of connective tissue that lines the inside of the marrow cavity and any canals passing through the compact bone. Both the periosteum and the endosteum membranes contain osteogenic cells. During growth or following injury, osteogenic cells can differentiate into bone-formin g osteoblasts or osteocytes.
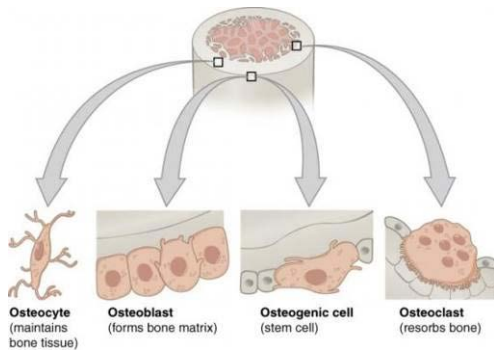
Figure 1 b Bone structure and bone cell types.

Four types of cells are found within bone tissue. Osteogenic cells are undifferentiated and develop into osteoblasts. When osteoblasts get trapped within the calcified matrix, their structure and function changes; they become osteocytes. Osteoclasts develop from monocytes and macrophages and differ in appearance from other bone cells.

Source: Boundless. "Cell Types in Bones." Boundless Biology. Boundless, 08 Jan. 2016. Retrieved 11 May. 2016 from https://www.boundless.com/biology/textbooks/boundless-biology-textbook/the-musculoskeletal-system-38/bone-216/cell-types-in-bones-816-12058/

Bone formation (osteogenesis) initiates with the process of cellular condensation, where dispersed mesenchymal cells migrate and proliferate [36] and subsequent bone development occurs in two different mechanisms: endochondral ossification (the formation of a cartilage template and its replacement by bone) and intramembranous ossification (direct differentiation of mesenchymal stem cells into osteoblasts), both processes involve the transformation of a pre-existing mesenchymal cells into bone tissue, and it take place in close proximity to vascular ingrowth.

The first type of ossification occurs during embryonic development and is involved in the development of flat bones in the cranium, various facial bones, parts of the mandible and clavicle and the addition of new bone to the shafts of most other bones. In contrast, bones of load bearing joints form by endochondral formation (Fig. 2).
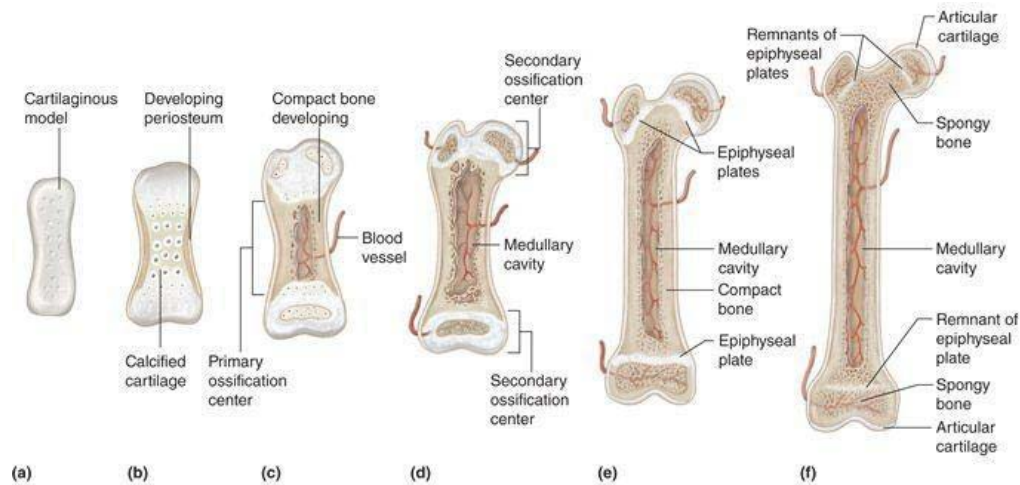
Figure 2   a schematic diagram of endochondral bone stages

(*a) Mesenchymal cells condense and differentiate into chondrocytes forming an avascular cartilage model of the future bone. (b) At the centre of condensation the chondrocytes cease proliferating and become hypertrophic. (c) Perichondral cells adjacent to the hypertrophic chondrocytes differentiate into osteoblasts forming a bone collar. The hypertrophic cartilage regulates the formation of mineralised matrix; the release of angiogenic factors to attract blood vessels and undergoes apoptosis. (d) The coordination of osteoblasts and vascular invasion form the primary spongiosa. The chondrocytes continue to proliferate with concomitant vascularization resulting in a coordinated process that lengthens the bone. Osteoblasts of the bone collar will eventually form cortical bone; while osteoblasts precursors located in the primary spongiosa will eventually form trabecular bone. (e) At the ends of the bone, secondary ossification centres develop through cycles of chondrocyte hypertrophy, vascular invasion and osteoblast activity. Columns of proliferating chondrocytes form in the growth plate beneath the secondary ossification centre. (f) Finally, expansion of stromal cells and hematopoietic marrow starts to take place in the marrow space.*
 From Marks and Hermey, 1996

Bone is a highly vascularized tissue reliant on the close spatial and temporal connection between blood vessels and bone cells to maintain skeletal integrity. During bone development, as well as, in the repair process tissue vascularisation is fundamental. The process of new vessels formation is called angiogenesis and occurs in the earlier stages of bone formation favouring growth factors import, mineral deposition and mesenchymal cells localization. There are a number of factors involved in neoangiogenesis but the main protagonists are Vascular Endothelial Growth Factors (VEGFs). VEGFs and their corresponding receptors are the key regulator s in the cascade of cellular e molecular events lead to the development of the vascular system, including vasculogenesis, angiogenesis and in the lymphatic vascular system formation [37]. It is already known the pivotal role of VEGF in the in skeletal growth [38] and repair [39]. The endothelium plays a significant role in the maintenance of homeostasis of the bone tissue providing growth factors, chemokines, cytokines and regulating movement of molecules and cells. The latter is very important for coordination signals forwarding in recruiting of cells or factors towards specific skeleton sites. This event cascade occurs during bone remodeling, in response to trauma or in pathophysiological conditions (rheumatoid arthritis and osteoarthritis) [40].

In the wound healing, as well as bone fracture repair, vascular system is closely involved. Indeed, bone healing is a complex biological process that follows specific regenerative steps also involving different biochemical events.

The trauma gives rise to an inflammatory response which is necessary for the healing to progress. The response causes the hematoma to coagulate in between and around the fracture edges and within the medullar canal forming a template for callus formation. The initial proinflammatory response involves secretion of tumor necrosis factor-α (TNF-α), interleukin-1 (IL-1), IL-6, IL-11 and IL-18. These factors recruit inflammatory cells and promote angiogenesis through the vascular endothelial growth factor (VEGF) production [41]. During this acute phase mesenchymal stem cells are recruited from bone marrow and surrounding soft tissues starting the regenerative stage where BMPs seem to have an important role. Adjacent to the distal and proximal ends of the fracture

both intramembranous and endochondral ossification give rise to the formation of a cartilaginous callus which later undergoes mineralization generating a hard callus [42]. In order to bone regeneration completing, the primary soft cartilaginous callus needs to be resorbed and replaced by a hard bony callus. For bone remodelling to be successful, an adequate blood supply and a gradual increase in mechanical stability is crucial [43] (Fig. 3).
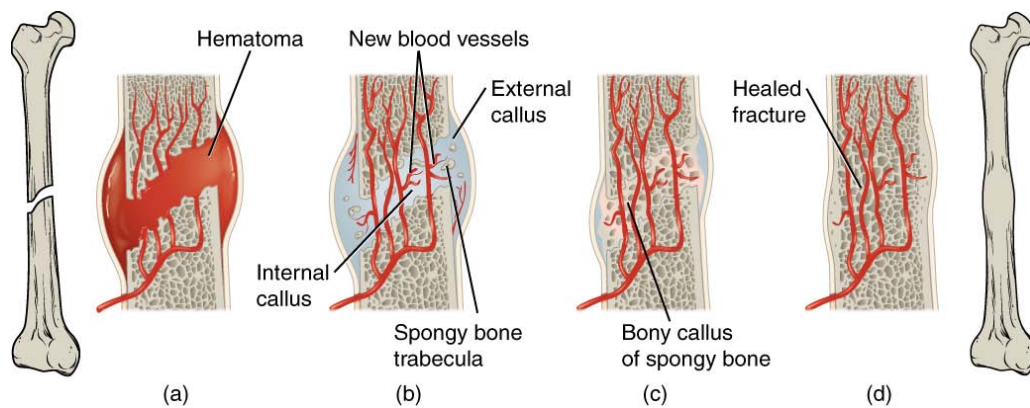

Figure 3 Steps of bone fracture healing*: (a) A fracture hematoma formation. (b) Internal and external calli formation. (c) Cartilage of the calli is replaced by trabecular bone. (d) Remodeling occurs. Source: http://philschatz.com/anatomy-book/contents/m46342.html*

2.2 REGENERATIVE MEDICINE: NEW PERSPECTIVES IN BONE REGENERATION

The repair of large bone defects remains a major orthopaedic challenge and the actual surgical procedures have not brought good long-time results and significant clinical outcomes. There is a plethora of different strategies to augment the impaired or "insufficient" bone-regeneration process.

Autologous bone graft is considered the gold standard but the need of bone harvesting improves site morbidity, for this reason allograft implantation bypass this problem nevertheless the integration ability and clinical outcomes are poorer than gold standard procedure. Several synthetic or biologic scaffold constructs have been employed in the development of tissue-engineered bone in these years but it is clear that needs more components to obtain and maintain the tissue.

Local strategies in terms of use of osteoinductive stimuli (bone marrow concentrate (BMC), platelet rich plasma (PRP), bone morphogenic proteins (BMPs) and growth factors combined with mesenchymal stem cells (from Bone marrow or other tissues, including muscle, periosteum, adipose tissue, vascular pericytes, dermis, and peripheral blood) have been largely investigated [44], more recently and, still under investigation, they are the "systemic approache" for the enhancement of bone repair, including growth hormones and parathyroid hormone (PTH) administration [45], and gene therapy [46] in an effort to overcome the limitations of the current methods to bone regeneration.

Tissue engineered bone constructs, therefore, should ideally have mechanical properties similar to native bone during the entire process of tissue repair and regeneration, especially when constructs are to be implanted in load-bearing sites.

Biological guidelines for bone tissue regeneration involve the interplay of four critical elements, namely: (1) osteoinductive growth factors (induce differentiation of stem cells to osteoblasts); (2) stem cells that respond to osteoinductive signals (osteogenic); (3) a scaffold that supports cellular attachment, proliferation, and ingrowth (osteoconductive

matrix) and (4) for graft host tissue functional integration and survival vascularization is an essential pre-requisite [47].

The development of a microvasculature and microcirculation is critical for the homeostasis and regeneration of living bone, without which, the tissue would simply degenerate and die. Vascular supply is necessary to assure efficient gas and nutrition exchange with all cells within the tissue but also for releasing of vascular growth factor (VSF) at the bone fracture site to induce repair process [48].

Currently, there are several approaches being utilized in order to vascularize bone grafts, and generally one or combination of three major principles can be followed. The main techniques are: 1) Bone grafts can be implanted into environments rich in vascular supply (subcutaneous, intramuscular, or intraperitoneal sites), where the constructs can be invaded with new vascular networks at their surfaces (In vivo pre-vascularization);
2) local delivery of angiogenic growth factors (VEGF, PDGF, and FGF). The combination of osteogenic (BMP-4) and angiogenic (VEGF) factors together with bone marrow stromal cells promoted bone formation at an ectopic site [49]. The combined delivery of cells, osteogenic and angiogenic factors resulted in a significant increase in the quantity of regenerated bone compared with any factor alone or any two associated factors;
3) vascularization of tissue engineered bone grafts seeding a co-culture of endothelial and osteogenic cells into the bone constructs engineered in vitro [47] (Fig. 4).
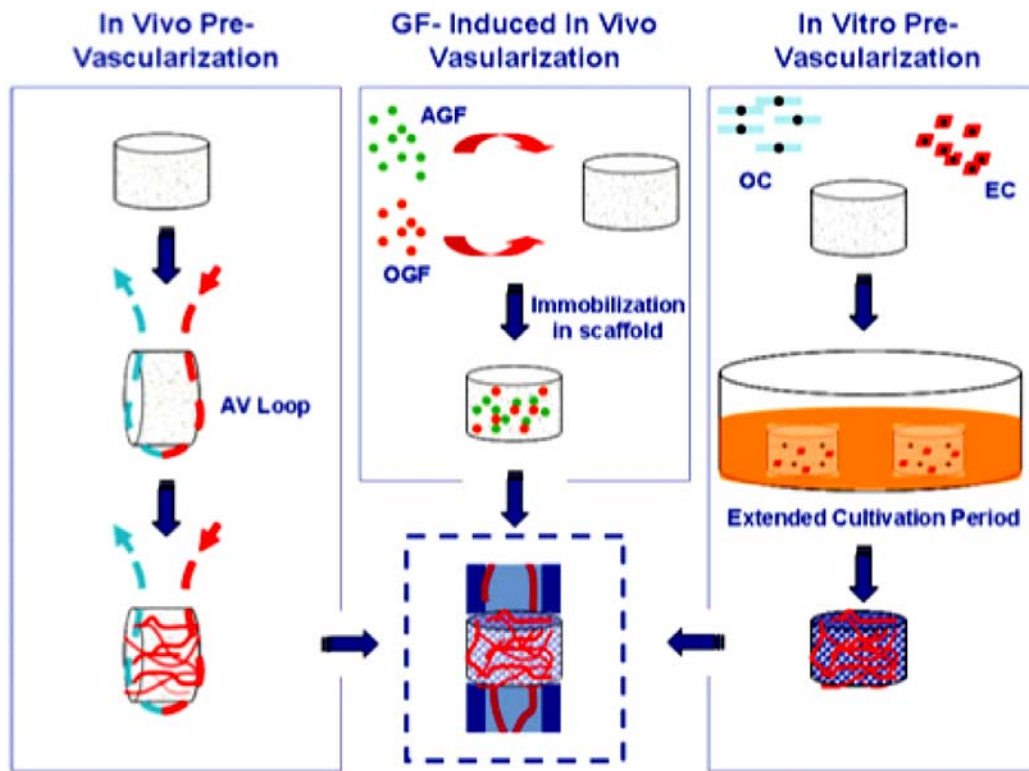
Figure 4 Approaches to Vascularizing Engineered Bone Scaffolds

Source: Fröhlich et al, Curr Stem Cell Res Ther. 2008.

CHAPTER 3
EXPERIMENTAL PROJECT

3.1 AIM OF THE STUDY

Aim of the present study is to investigate the results of an innovative technique based on a bio-composite made of allografts, BMSCs and vascular supplement for the reconstruction of large bone defects. This technique has been developed in order to give answer to all that complex and difficult situations that lead to a long bone critical size defect, where the surgical procedures at the state of the art are not satisfying. In order to pursuit this goal an animal model has been set up taking into account the type of tissue to be repaired, the amount of bone loss to be created, the state of the art knowledges in biology and regenerative medicine.

CHAPTER 4

MATERIALS AND METHODS

It was decided that for this aim the rabbits would have been the most appropriate animal model, in particular the radius bone. Rabbit in fact is one of the most commonly used animal models, and it ranks first among all the animals used for musculoskeletal research. It was reported that there were similarities in bone mineral density and the fracture toughness of mid-diaphyseal bone between rabbits and human. Besides that, in comparison with other species, such as primates or some rodents, rabbit has faster skeletal change and bone turnover. In particular, the anterior limb of the rabbit is a low weight bearing limb and has an extremely limited pronation-supination movement, which constitutes an optimal characteristic to test bone substitute since there's no necessity of strong hardware to fix the graft to the healthy bone. Furthermore, rabbits are easily available, and easy to house and handle.

The study was conducted in compliance with Italian and European laws concerning animal experiments. The research protocol was approved by the Ethics Committee of 'Rizzoli Orthopaedic Institute and authorized by Italian Ministry of Health according to Legislative Decree 116/92 and was performed according to Legislative Decree 26/2014.

4.1 SURGICAL PROCEDURE

A total of 24 HYCR adult rabbits (Harlan Laboratories s.r.l., Udine, Italy), weight 3.0±0.4kg, were employed and housed, in accordance with the Recommendations 2007/526/CE, at the following environmental conditions: individual cages, standard diet with long-term maintenance pelleted feed (Mucedola s.r.l., Settimo Milanese, Italy) and water ad libitum, temperature 20.5 ± 0.5 °C and relative humidity $55 \pm 10\%$. After the period of quarantine, the animals were randomized in the experimental groups as following (Fig.5):

The 24 rabbits have been divided into 2 groups:
  - Group 1 (#12): allogenic bone graft (left radius) / allogenic bone graft + vascular pedicle + autologous bone marrow concentrate (right radius)
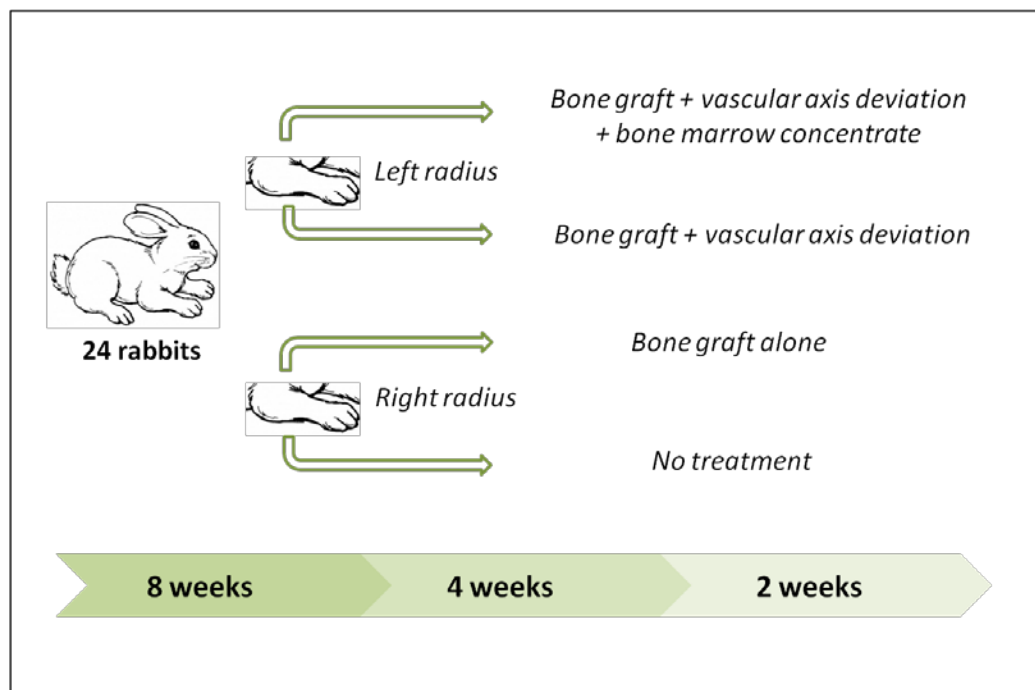 - Group 2 (#12): sham operated (left radius)/ allogenic bone graft + vascular pedicle (right radius)

Figure 5 *Experimental design of the study*

For each group, 3 experimental times have been set up: 8, 4 and 2 weeks (4 animals for each time). The bone used as graft was previously collected from an uncorrelated study. After premedication with intramuscular injection of 44 mg/kg ketamine (Imalgene 1000, Merial Italy SpA, Assago-Milano, Italy) and 3 mg/kg xylazine (Rompun 25 ml, Bayer SpA, Italy), general anesthesia was induced and maintained with the administration of a gaseous mixture (O_2/air: 60%/ 40%), in spontaneous ventilation by administration of sevoflurane 2-3% (Sevoflurane, Baxter SpA, Rome, Italy).

The surgical procedure was performed after bilateral anterior leg shaving and washing with antiseptic solution of the rabbits.

For the rabbits in which the bone marrow was to be added to the procedure, bilateral iliac crest region of the rabbit was shaved and cleaned. An initial 5cc of whole bone marrow was harvested from the posterior iliac crest with the addition of anticoagulant solution and sent to the lab for concentration; the bone marrow was stratified on gradient of density (Ficoll) and the obtained mononuclear cell fraction washed and returned to operating room.

A longitudinal skin incision was then performed in the anterior leg of the rabbit in the antero-medial aspect, in the area between radius and ulna. Muscles were retracted and the median vascular bundle was isolated and protected. The midshaft of the radius was then exposed, and a 1,5 cm segmental defect (Fig. 6) was made over the midshaft of the rabbit radius using an electric saw, and periosteum surrounding the defect was completely removed.
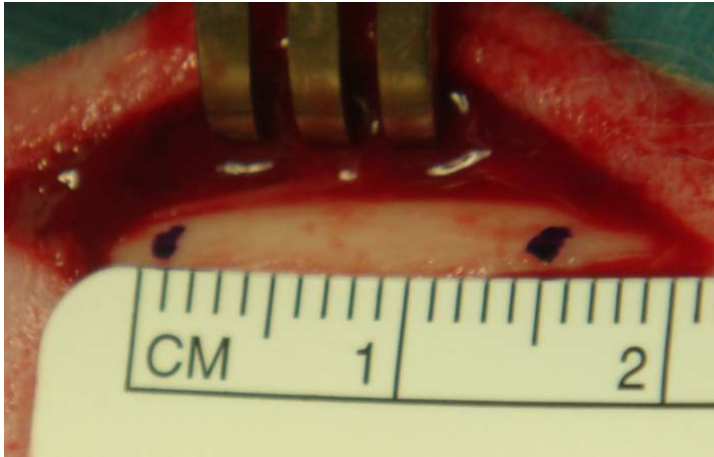
Figure 6 *1.5 cm of the radial shaft are marked and subsequently removed*

In right radius of one experimental group this constituted the control group and the defect was not filled with any graft. The muscular layer, the subcutaneous tissue and the skin were sutured with appropriate stitches, medicated and dressed.

In right radius of the other experimental group the bony gap was filled with a cylindric allograft, countured from a rabbit radius previously explanted from animals which has undergone another experimental protocol and stored at -80°, as a normal procedure for human bone allograft. The graft was shaped in order to fill the gap with press fit technique, and was secured to the original bone with two 2.0 polysorb stitches or two metallic wire circlages.

In left radius of one experimental group the gap was filled with an allograft with a vascular deviation inside: the cylindrical graft was shaped with an electric burr, performing a longitudinal complete incision on one side opening longitudinally the graft canal. This permitted to the median vascular bundle to be positioned inside the graft without a microsurgical anastomosis. In order to not compress the vascular bundle entering and exiting from the graft, on the other side of the graft two small longitudinal incisions were performed (Fig. 7).
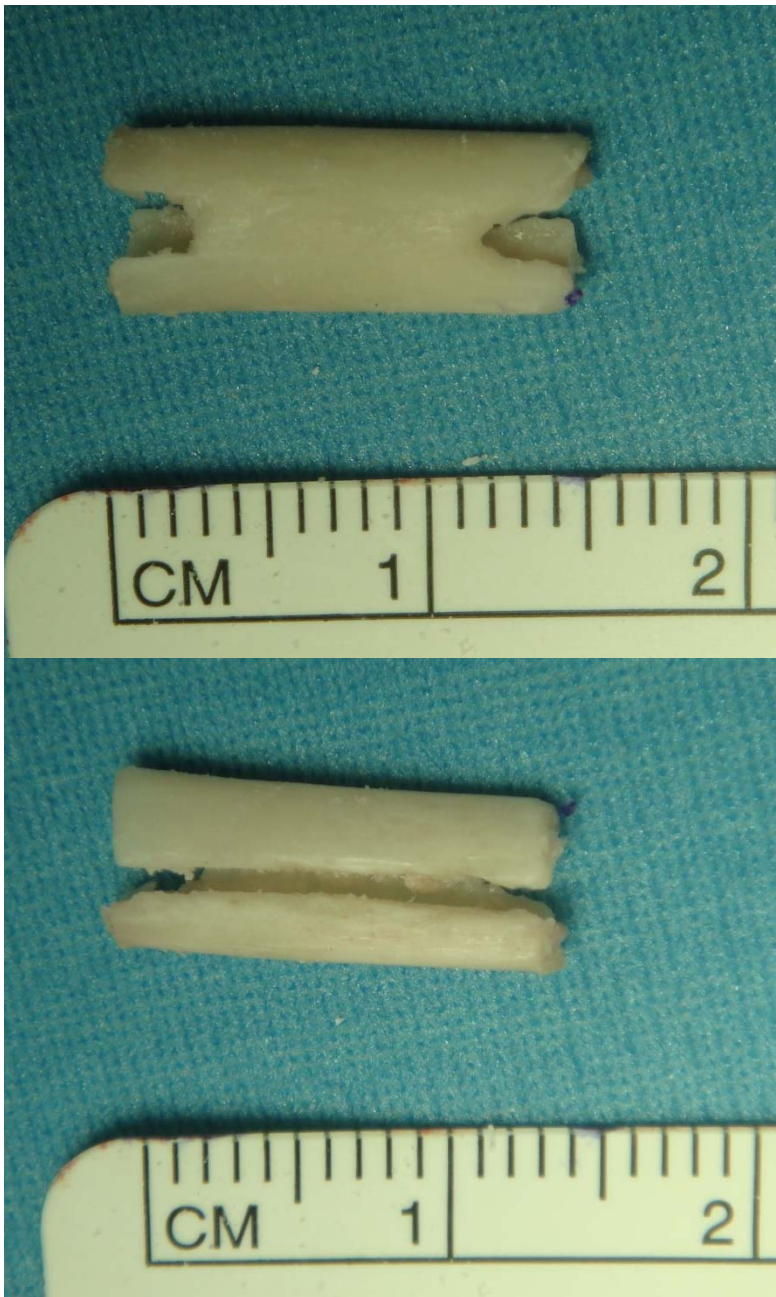
Figure 7 *The graft to be inserted is shaped in order to fit the vascular bundle at its inside without compressing it.*

The graft with the vascular bundle at its inside was then press-fit positioned into the defect and fixed as described above, taking care not to overstretch the bundle and double checking that the vessels were not compressed (Fig. 8,9).

Figure 8 *The median vascular bundle is inserted in the allograft from the longitudinal opening*

Figure 9 *The allograft with the vascular bundle is than press-fit positioned in the bony gap and subsequently secured with suture or metallic circlages.*

In the other group of left radius, a biomaterial was positioned around the described construct: a scaffold made of equine type I collagen (BIOPAD®, Novagenit, Trento-Italy) loaded with 1 ml of autologous bone marrow previously harvested and concentrated. At this point the muscular layer was closed covering the whole construct, and a standard closure was performed as previously described (Fig. 10).
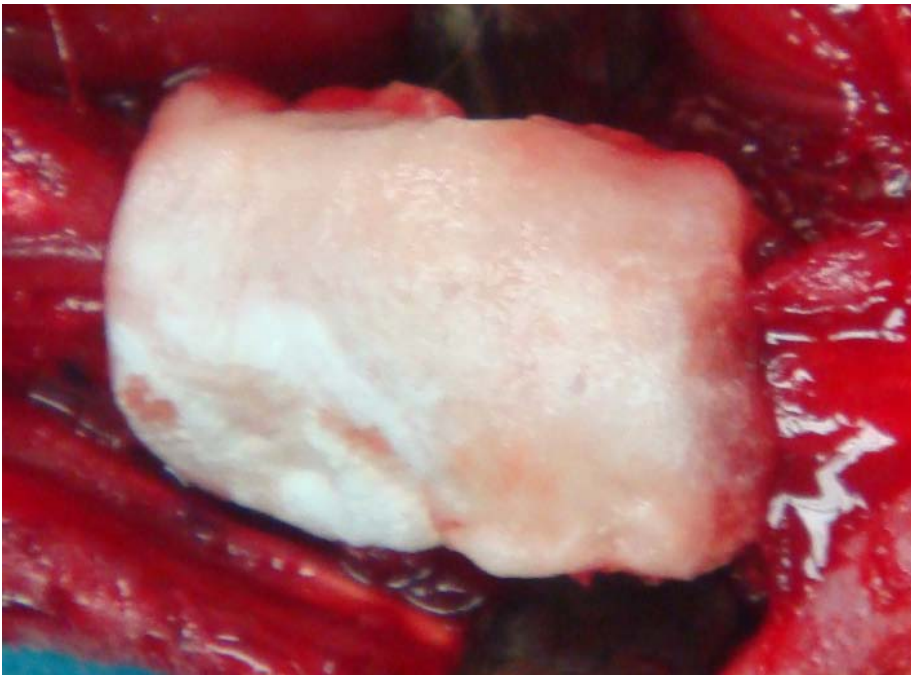

Figure 10 *The BIOPAD with the bone marrow concentrate is than positioned onto the graft, wrapping the entire construct. The muscular layer is than sutured onto the implant and a standard closure is performed.*

4.2 POSTOPERATIVE CARE

Postsurgical rabbits were housed individually cage, with food and water ad libitum. Intramuscular administrations of antibiotics Flumequine (Flumexil, Fatro SpA, Bologna-Italy) for 4 days and analgesics, 80 mg/Kg of sodium metamizole (Farmolisina, Ceva SpA, Monza-Italy) and a Fentanyl transdermal patches was applied in the external surface of the hear for 3 days (Matrifen 25µg/72h, Grunenthal Italia Srl). The rabbits were regularly monitored for signs of infection and instability of fixations. Dressing was changed whenever necessary.

At the end of experimental time, rabbits were kept in deep sedation (ketamine and xylazine i.m.) to allow bone marrow harvesting from the iliac crest and pharmacological euthanasia through intravenous injection of 1 ml of Tanax (Hoechst AG, Franfurt-am-Main, Germany). After macroscopic examination of the bone and surrounding soft tissue, the radius segments were removed and an overall macroscopic assessment of the tissue state was made (presence of hematomas, edema, inflammatory reactions or necrosis).

4.3 CELL CULTURES, RABBIT BONE MESENCHYMAL STEM CELLS (rBMSC) CHARACTERIZATION AND SCAFFOLD SEEDING

4.3.1 rBMSC isolation and expansion

Rabbit bone marrow was harvested by iliac crest from all the animals. After 1:4 dilutions in phosphate buffer saline (PBS), the sample was stratified on density gradient medium (Ficoll-Paque, density 1.077g/ml, Sigma-Aldrich, MO, USA), to obtain mononuclear cells (MNCs).They were then twice washed with PBS, counted in Neubauer chamber and seeded in flasks at a density of approximately $4x10^5$ cells/cm^2 in a basal medium (BM) composed by Dulbecco's Modified Eagles Medium (DMEM, Sigma-Aldrich, St.Louis, MO, USA), 10% Fetal Bovine Serum (FBS, Lonza, Verviers, Belgium), 100U/ml penicillin, 100mg/ml streptomycin (Gibco, Life Technologies, Carlsbad, CA, USA) and 5 µg/ml plasmocin (Invivogen, San Diego, CA, USA). Cultures were maintained at 37°C, in a 5% CO_2 /air humidified atmosphere to select rBMSC by means of adhesion to plastic substrate and expanded until the 2th passage. Then, they were detached with 0.05% Trypsin/EDTA and used for all the experiments.

4.3.2 rBMSCcharacterization: trilineages differentiation

For adipogenic differentiation, the cells were seeded at the density of $5x10^3$ cell/cm^{2}in 24 well plates and maintained up to 2 weeks in adipogenic medium (AM), consisting of BM added with insulin (10µg/ml), isobutylmethylxanthine (500µM), indomethacin(100µM), dexamethasone (1µM). Adipogenic differentiation was assessed using an Oil Red O stain as indicator of intracellular lipid accumulation. Prior to staining, the cells were fixed for 10 min at room temperature (RT) in 4%

paraformaldehyde, extensively washed with deionized water, and incubated at RT for 5 min in 60% isopropanol solution. After washing with deionized water, a 1.8% Oil Red solution in 60% isopropanol was added to culture for 15 min at RT. At the end of incubation, significant imagines were captured to appreciate red lipid vacuoles by using Eclipse TiU inverted microscope (NIKON Europe BV, NITAL SpA, Milan, Italy).

For chondrogenic differentiation, 2.5×10^5 cells per tube (Sarstedt, Nümbrecht, Germany) were pelleted in micromasses (10 minutes, 160g) and kept in 1 ml of chondrogenic medium (CM): differentiation basal medium-chondrogenic (POIETICS, LONZA, Verviers, Belgium), added with suitable supplements and 10% FBS (POIETICS, LONZA, Verviers, Belgium). The micromasses, which represent the recommended 3D-system to induce a correct chondrocyte differentiation, were cultured for a month. Micromasses as control were set up in BM.

At experimental endpoint, chondrogenesis was confirmed using histological staining and Glicosaminoglycan (GAG) quantification. The micromasses were in addition analyzed for extracellular chondrogenic matrix formation in term of glycosaminoglycans (GAGs) synthesis. The assay was performed by measuring the reaction between GAGs and 1,9-dimethylmethylene blue (DMMB) reagent (Sigma–Aldrich). The samples were digested overnight with 0.3mg/ml papain solution in a phosphate/EDTA buffer, pH 6.5, at 65°C, added with DMMB solution to develope a GAG-dye complex, and spectrophotometrically read at 525nm (iMARK Microplate Reader, Bio-Rad). Total GAGs content was extrapolated referring to a standard curve set up with shark chondroitin sulfate (Sigma-Aldrich).

For osteogenic differentiation, the cells were seeded at the density of 5×10^3 cell/cm^2 in 24 well plates and maintained up 14 days in osteogenic medium (OM) consisting of BM added with 50μg/ml ascorbic acid 2P, 7 mM β-glicerophosphate and 10^{-7}M dexamethasone (Sigma Aldrich).

To quantify the osteogenic differentiation, intracellular alkaline phosphatase (ALP) activity was evaluated by reading the kinetics of p-nitrophenyl phosphate hydrolysis in the presence of ALPase. The developed color was spectrophotometrically read at 405

nm (iMARK Microplate Reader, Bio-Rad) and the concentration of the 4-nitrophenol product was calculated referring to a standard curve. All the chemicals were purchased from Sigma-Aldrich.

In addition, to observe and quantify the Ca/P deposition, cells were fixed with 4% paraformaldehyde for 15 min at RT and stained for 1 hour with a 2% ARS solution, pH 4.2. The cultures were then rinsed with distilled water until clear. Representative images were captured using Eclipse TiU inverted microscope at 10x magnification. ARS was subsequently eluted using a solution of 10% w/v cetylpyridinium chloride in sodium phosphate 10 mM, pH 7 (Sigma-Aldrich). The absorbance of the resulting solution was measured at 570 nm (iMARK Microplate Reader, Bio-Rad, Hercules, CA) and ARS concentration was obtained by referring to a standard curve [50].

All experiments were performed by setting up both the conditions of differentiation and control, in three independent replicates.

4.3.3 Gene expression analysis

At 24 hours, 1 week and 2 weeks, total RNA was extracted from the cultures differentiating toward osteoblast lineage (and relative controls) with a phenol-chloroform method using Trizol reagent (Life Technologies) and reverse transcribed using the Superscript Vilo cDNA synthesis kit (Life Technologies), following the manufacturers' instructions. cDNA was quantified by using Quant-iT Pico-Green dsDNA assay kit and diluted to the final concentration of 5 ng/µl.

Quantitative polymerase chain reaction (qPCR) analysis was performed using the QuantiTect SYBR green PCR kit (Qiagen, Hilden, Germany) in a Light Cycler 2.0 Instrument (Roche Diagnostics).

The protocol included a denaturation at 95°C for 15 minutes, 30-50 cycles of amplification (95°C for 20s, 55°C for 20s and 72°C for 20s) and a melting curve analysis to check for amplicon specificity. Ten nanograms of each sample were tested in duplicate. The mean threshold cycle was used for the calculation of relative expression using the $2^{-\Delta\Delta Ct}$ method, against GAPDH as the reference gene and using the CRL condition at 24h as the calibrator.

4.3.4 Scaffold seeding

The same material employed for *in vivo* implants has been tested *in vitro* for cell adhesion and viability. Briefly, BIOPAD® scaffold was placed in 24-well plates, prewetted with OM for 1 hour and seeded dropwise with $2x10^5/cm^2$rBMSC suspended in 30µl of medium. The constructs were then incubated for 3h to allow cell attachment and scaffold colonization, before adding the remaining OM volume.

After 24 hours, 7 and 14days the cell viability was observed by the fluorescent labeling LIVE/DEAD® assay (Molecular Probes, Eugene, OR, USA), according to the manufacturer's instructions. Samples were visualized using Eclipse TiU inverted microscope equipped with an epifluorescence setup: excitation/emission setting of 488/530 nm to detect greenfluorescence (live cells) and 530/580 nm to detect red fluorescence (dead cells).

At the same time points the constructs were observed also by histology (see below). Three replicates of constructs were set up, using as many bone marrow samples.

4.3.5 Cocultures

Primary rabbit vein endothelial cells (rEC, Cell Biologics, Chicago, USA) were seeded on the bottom of 12 well multiplate at the density of $1.5x10^4$cell/cm^{2}after well precoating set up with gelatin. Separately, rabbit rBMSC were seeded dropwise on BIOPAD® scaffold at the density of $2x10^5$ cell/cm^2 after 2 hours of scaffold prewetting in complete medium. Each BIOPAD® scaffold were placed inside a cell culture insert (Millicel 0.4μm pore-size, PCF, 12 mm diameter, Millipore, Tulagreen Carrigtwohill, Co. Cork, Ireland). Twenty-four hours after seedings, to allow endothelial cells adhesion to plastic substrate and rBMSC to the scaffold, co-cultures were set-up by transferring the culture inserts in the wells containing the rEC. The medium was a mixture of OM and complete medium EBM-2 (Clonetics LONZA, Walkersville, MD, USA) and was replaced twice a week. In the same multiplates, also single cultures: rBMSC on BIOPAD scaffold, endothelial cells alone, were set up. All cultures were maintained until 14 days. After 24 hours, 7 and 14days the cell viability was observed by the fluorescent labeling LIVE/DEAD® assay as described in the previous section.

4.4 X-RAY AND MICROTOMOGRAPHY

Standard 2 poses X rays of the operated forearms were taken at the sacrifice times. The retrieved forearm bone samples were scanned with the high-resolution microtomography system Skyscan 1176 (Bruker Micro-CT, Belgium) using a nominal resolution of 35 µm. The source voltage was set on50kV with a current of 500µA and an aluminum filter 0.5mm thick was interposed between the x-ray source and the sample. Each sample was rotated until 180° with a rotation step of 0.5° and a frame averaging of 2. The images obtained from acquisition were later reconstructed by the software NRecon (version 1.6.10) with corrections for alignment, depended on acquisition, beam hardening and ring artifact reduction. The images resulted jpg images had 1000X1000 pixels with a pixel size of 35 µm.

Quantitative 3D analyses were carried out with CTAn software (version 1.15.4, Bruker Micro-CT, Belgium) in a cubic Volume of Interest (VOI) of 20x20x20 mm defined in each samples in order to keep the defect /graft in the central position.

The following morphological parameters were evaluated:

- Callus density, *Cl.V/TV* (%); defined as the ratio between Callus Volume in mm^3 (*Cl.V*) including voids and the defined VOI (*TV*) in mm^3;

- Callus Index, *Cl.Ind* (%); defined as:

$$\frac{(Cl.V - Cl.V_{tissue})}{Cl.V} \times 100$$

where *Cl.V* is the Callus Volume as defined above and $Cl.V_{tissue}$ is the Callus Tissue Volume in mm^3, defined as the callus tissue volume, exclusive voids, e.g. pores and gaps;

- Volumetric Bone/Implant contact *VBIC* (%,); defined as the ratio between the area of the bone graft (implant) in the direct contact with the surrounding bone and the total area of the graft.

In addition, 3D models of the samples inside the VOI were created in order to assess three-dimensionally the quality of the treatments.

4.5 HISTOLOGY AND IMMUNOHISTOCHEMISTRY

4.5.1 Histological processing of forearm bone samples

Left and right forearm bone segments were harvested from each rabbits and processed for paraffin embedding. More in details, samples were fixed in 10% neutral buffered formalin (Sigma-Aldrich, Saint Louis, Missouri, USA) for at least 24 hours at room temperature. After rinsing in running tap water, samples were decalcified in 5% solution of formic (ACEF, Fiumicino, Rome, Italy) and nitric acid (Sigma-Aldrich, Saint Louis, Missouri, USA) for 20 days at 37°C and then extensively rinsed in distilled water. Each radius was cut along the major axis to help the inclusion and dehydrated in increasing ethanol solutions (Panreac AppliChem, Barcelona, Spain) for 1 hours each (70%, 95% twice, 100% twice), to remove the aqueous component and facilitate the penetration of the embedding medium, and defatted in xylene (VWR International, Milan, Italy). After overnight infiltration in liquid wax (56°C), samples were finally embedded in paraffin (Sigma-Aldrich, Saint Louis, Missouri, USA). From tissue blocks, thin histological section (5 μm thick) were obtained by a semi-automated microtome (MicromH340E,

Germany) and stained with Haematoxylin (Sigma-Aldrich, Saint Louis, Missouri, USA) and Eosin (Bio-Optica, Milan, Italy) (H/E). Images of each section were acquired with digital scanner at different magnification.

4.5.2 Immunohistochemical tests on forearm bone samples

Three slides from each specimen were selected to be tested for Vascular Endothelia Growth Factor (VEGF), Slices were dewaxed with consecutive steps in xylene and in decreasing graded ethanol solutions (5 minutes each) until PBS rinsing for 10 min. After permeabilization by incubation in 0.3 % hydrogen peroxide in PBS solution for 15 min, slides were pre-treated for antigen unmasking with 0.2 % Pronase (Sigma-Aldrich, Saint Louis, US-MO) solution in PBS for 30 min at 37 °C. After washing, the slides were incubated at room temperature for 1 hour with Blocking Serum (Vectastain Universal Quick Kit, Vectors Laboratories, Burlingame, US-CA) in order to prevent nonspecific bindings, then incubated overnight at 4 °C with specific rabbit polyclonal antibody against VEGF (Novus Biologicals, Littleton, US-CO), at a concentration of 1:100. After rinsing in PBS, slides were incubated with a universal HRP-conjugated secondary antibody and Streptavidin/Peroxidase complex (VECTASTAIN® Universal Quick Kit Concentrate). The reactions were finally developed using Vector NovaRed Substrate Kit for Peroxidase (Vectors Laboratories, Burlingame, US-CA).

As negative controls slides treated omitting the primary antibody were used, in order to check proper specificity and performance of the applied reagents.

4.5.3 Histological processing of chondrogenic micromasses and BIOPAD® seeded scaffolds with rBMSC

At the end of *in vitro* tests experimental time, micromasses and BIOPAD® seeded scaffolds were fixed in 10% neutral buffered formalin for 30 min, washed in distilled water and dehydrated in graded ethanol series 30 minutes for each steps. Finally, they were embedded in paraffin and the obtained blocks sectioned in the trasversal plane. A series of 5 µm section were obtained and analyzed for histology after staining with Hematoxylin-Eosin to appreciate cellularity and extracellular matrix organization of micromasses and the scaffold seeding and cells distribution for BIOPAD® seeded scaffolds.

4.6 STATISTICAL ANALYSIS

Statistical analysis was performed using the IBM® SPSS® Statistics v.23 software. The tested hypotheses were: (1) the presence of bone grafts is able to improve the healing of the critical size defect realized into the radio in comparison to untreated; (2) the deviation of vascular axis inside the medullary cavity of bone graft increased the healing process in comparison to bone graft alone; and (3) what is the advantage to add a collagen based scaffold over the bone graft with vascular axis inside. After having verified that data did not present a normal distribution (Kolmogorov Smirnov test), the Student's *t* test was used to compare data by creating 15,000 bootstrap samples from the entire data set and repeating the estimation process. Bias corrected and accelerated (BCa) 95% confidence intervals (CI) were obtained using bootstrap method of the corresponding sampling distributions. Data are reported as Mean, BCa 95% CI at a one tailed *p*-value < 0.05.

CHAPTER 5
RESULTS

5.1 MACROSCOPIC ASSESSMENT

All the treated animals reached the expected experimental times without any clinical complications.

Mascroscopic evaluations did not highlight any evidence of inflammation, infection, hematoma, edema or reaction in the tissues surrounding the radius.

The native structure and architecture of the bone around the implant appeared preserved, as well as the adjacent segment of ulna. The surgical procedure for the insertion of bone graft did not alter the physiological structure of the anatomical region. In some cases, the formation of a synostosis between radio and ulna was noted.

The integration of the graft at both the extremities of the defect was still incomplete, however the graft remained generally in place even though in some cases it was not completely aligned.

Mostly at the experimental time of 8 weeks, contact areas between the graft and the surrounding bone can be observed.

5.2 CELL CULTURES, RABBIT BONE MESENCHYMAL STEM CELLS (RBMSC) CHARACTERIZATION AND SCAFFOLD SEEDING

All the rBMSC samples demonstrated the ability to give rise to adipocytes, chondrocytes and osteoblasts (Fig. 11). The rBMSC cultures differentiating to adipocytes showed an intracellular accumulation of lipid droplet (Fig. 11 a,b); those to chondrocytes, under micromass conditions, presented GAG deposition and cellular organization in the typical matrix lacunae (Fig. 11 c,d); and those to osteogenic displayed the typical mineralization nodules (Fig. 11 e,f).

Furthermore, the biochemical evaluation performed by DMMB method confirmed a significant ($p < 0.05$) higher amount of GAG in the matrix of the micromasses maintained in CM (2565 ng, 356-5013) in respect than those grown in BM (125 ng, 68-181). The osteogenic differentiation was partially confirmed by the synthesis of ALP that showed a significant higher production of intracellular ALP in OM than BM after 7 (OM: 138.4μmol, 98.5 – 178.4; BM: 52.7μmol, 47.3 – 68.2; $p < 0.05$) and 14 (OM: 116 μmol, 92 - 143; BM: 87 μmol,58 - 112; $p = 0.09$) days of cultures. The Alizarin Red histochemical staining followed by cetylpyridinium quantification detected the calcium deposition (*ref. Y. D-C Halvorsen, Tissue Engineering, 2001),* that resulted higher ($p < 0.05$) in the OM (297 nmol, 130-502) than BM (97 nmol, 57-147) after 28 days of culture.
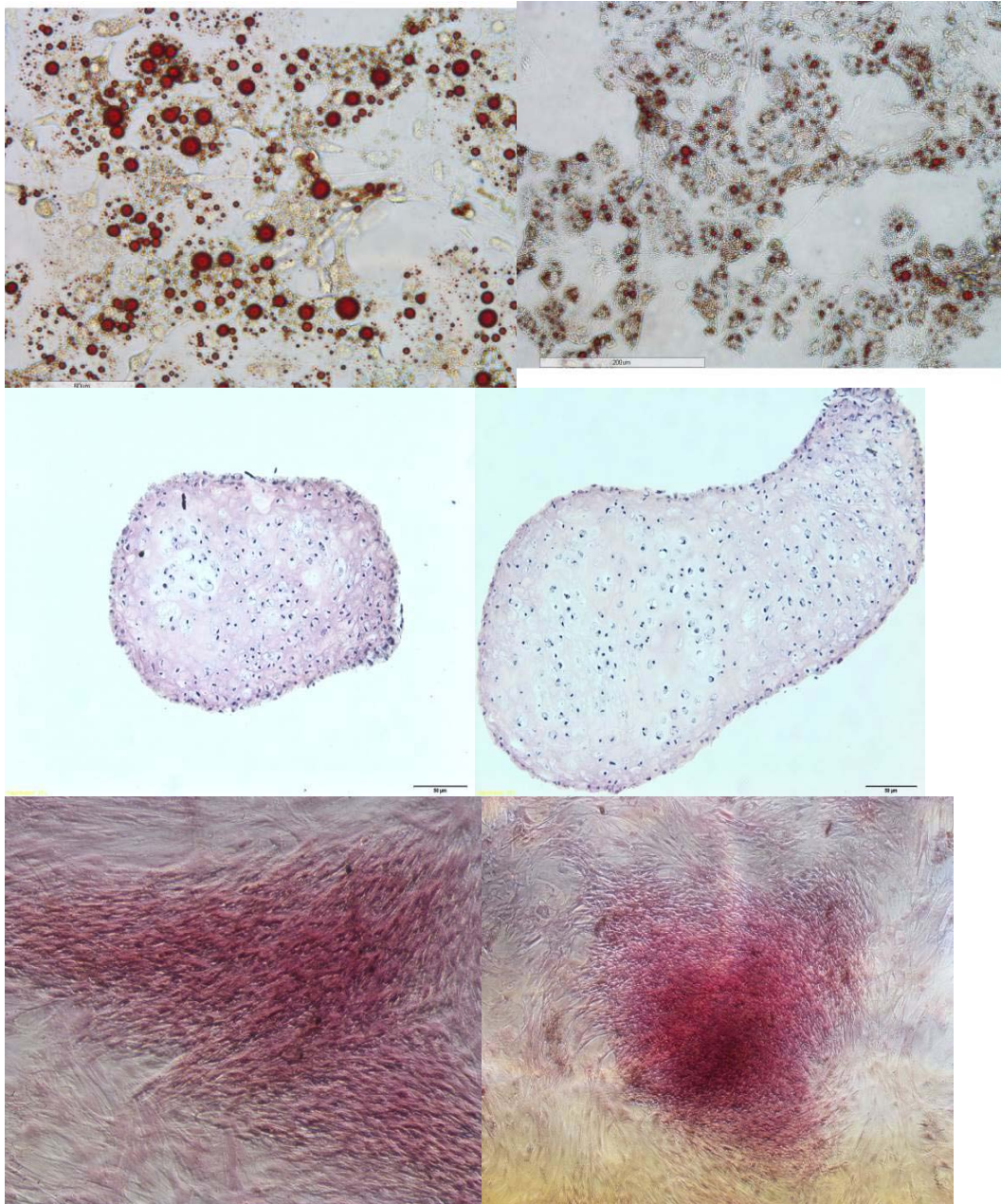
Figure 11 *Trilineages differentiation of BMSC cultures. a,b (magn. 40x): adipogenic differentiation. Evident lipid droplets after 2 weeks of cultures. c,d (magn. 20x): condrogenic differentiation. Histological images of micromass sections after 1 month of culture. e,f (magn.10x, 4x): osteogenic differentiation. Alizarin Red staining for the evaluation of calcium-rich deposits after 2 weeks of culture.*

By means of RT-PCR was evaluated the expression of the main genes of the osteoblast differentiation (Fig. 12). *Col1a1* and *Alpl* were significantly ($p < 0.05$) upregulated at 14 days in comparison to the other experimental times. On the contrary, *Il1a* was significantly down regulated after 24 hours ($p < 0.005$).

In order to observe *in vitro* the adhesion ability of rBMSC to the biomaterial employed *in vivo*, fluorescent staining was used. Qualitative results showed a great cell density on the scaffold surface, but it has been possible to appreciate also the cell infiltration inside the first thickness layers. Thanks to the differential staining, it was possible to distinguish live and dead cells, and to note that the totality of cells was alive, spread and organized at 24 hours such as at 2 weeks. Results were supported by histological analysis, which showed the distribution of cells all inside the material (Fig. 13).

Finally, the cocultures obtained by seeding rBMSC on the scaffold in presence of rEC on the same well bottom revealed a positive influence of the endothelial cells on the rBMSC proliferation (Fig. 14). This evaluation with fluorescent staining showed in fact an increase in the number of the mesenchymal cells when stimulated by rEC in comparison to cell cultured alone.
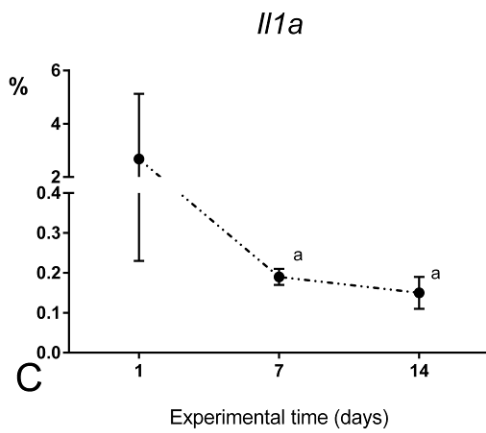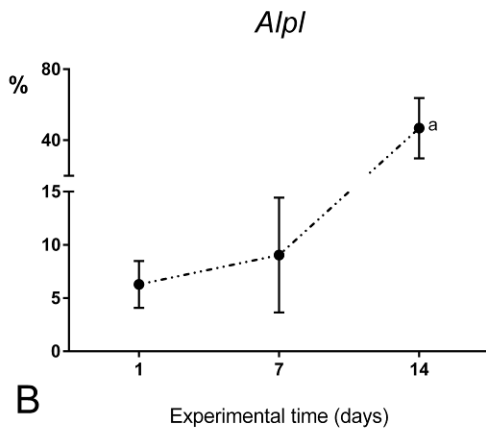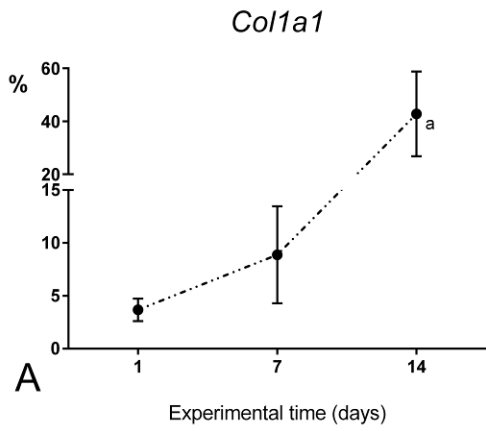
Figure 12 *Gene expression results of Col1a1 (A), Alpl (B), Il1a (C). Non parametric Student t test (bootstrap) (a, p < 0.05): 14 days versus other experimental time points for Col1a1 (a), Alpl (b); 1 days versus other experimental time points for Il1a.*
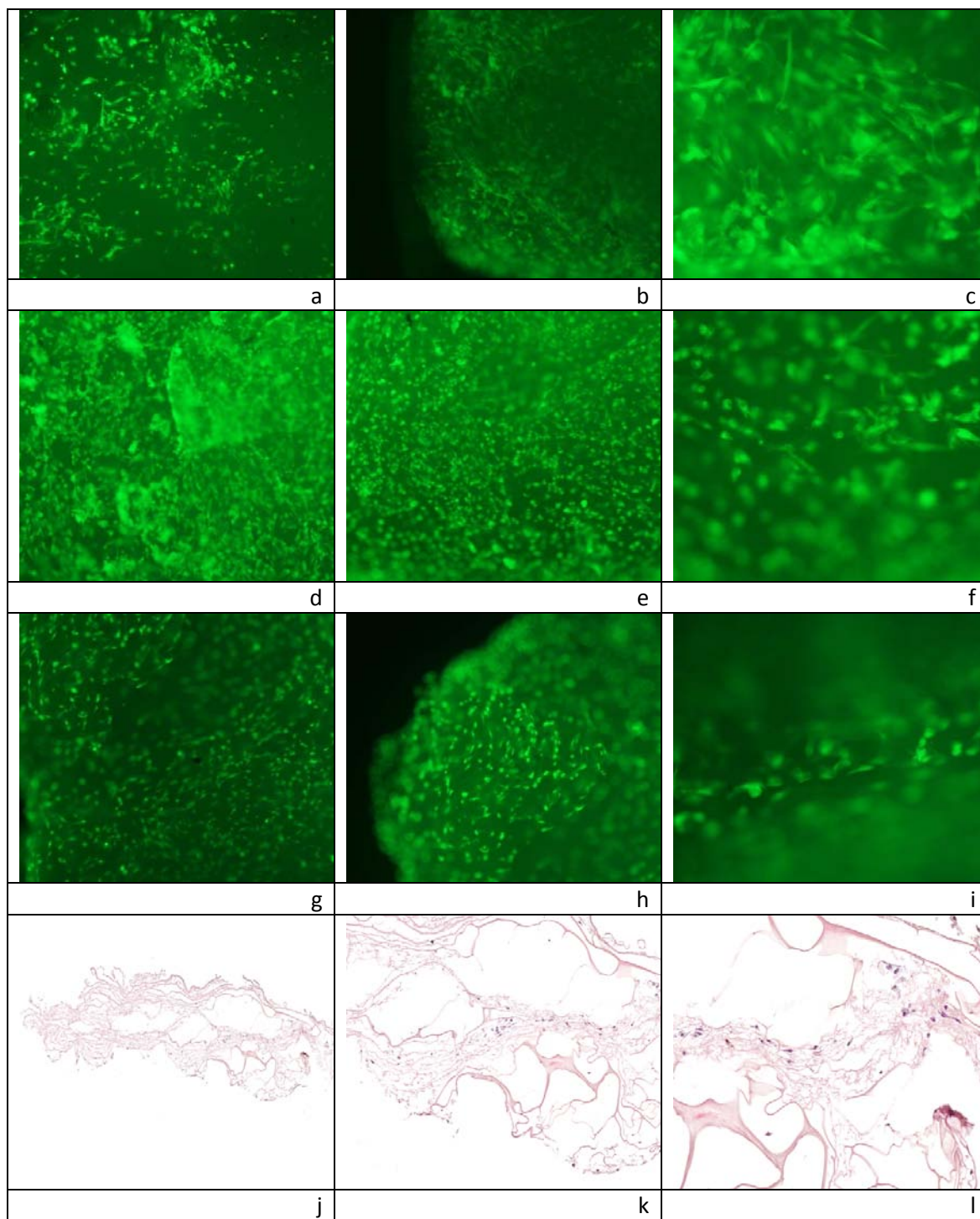
Figure 13 *Scaffold colonization by BMSCs labeled with fluorescent LIVE/DEAD® staining at 24h (a,b,c), 1 week (d,e,f) and 2 weeks (g,h,i), and histological images of seeded scaffold stained with Hematoxylin/Eosin at 24h (j), 1 week (k) and 2 weeks (l). Magn. 4x (a,b,d,e,g,h) 5x (j), 10x (c,f,k), and 20x (l).*
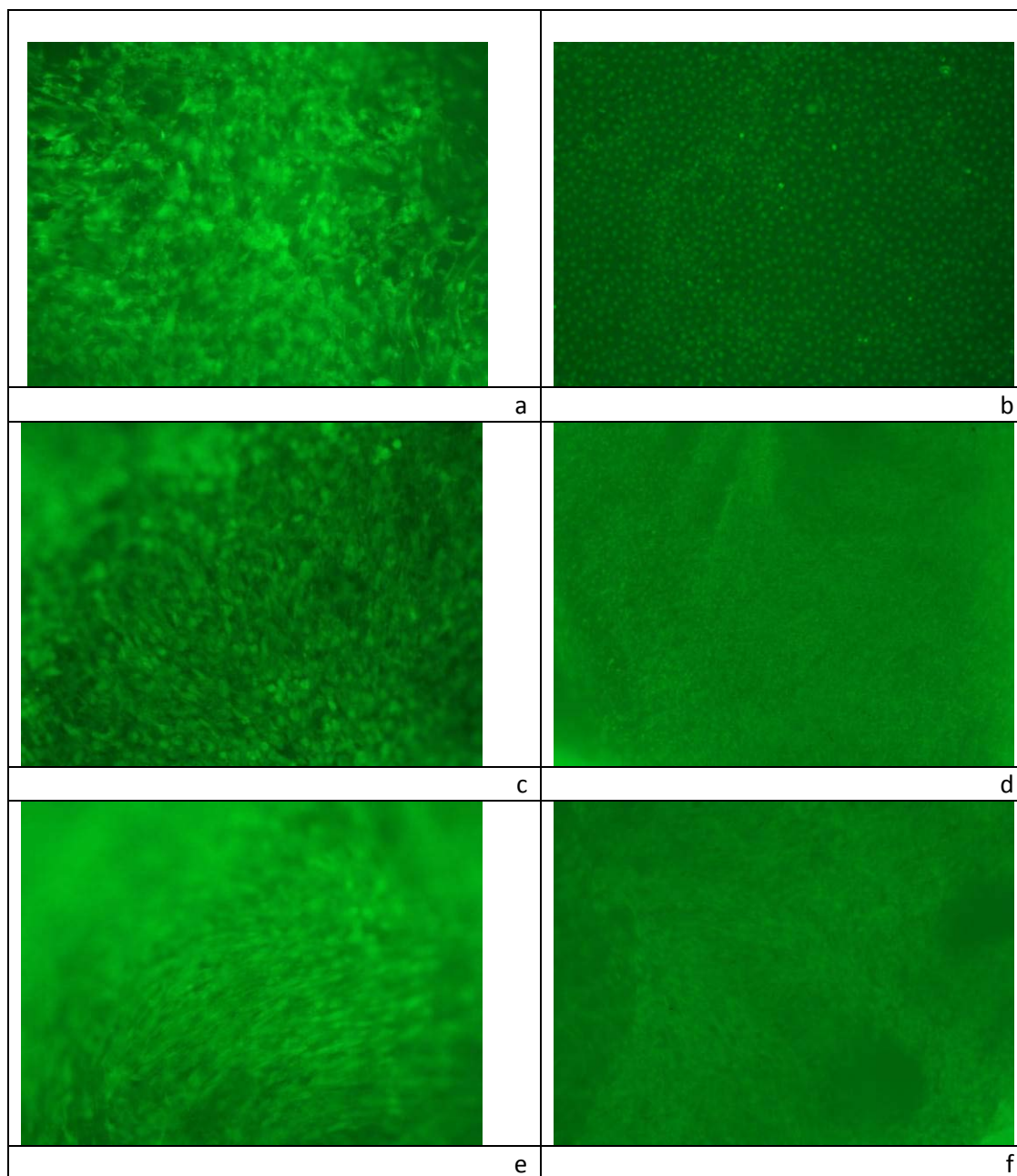
Figure 14 *Scaffold colonization by BMSCs labeled with fluorescent LIVE/DEAD® staining at 1 week (a,b), and 2 weeks (c,d,e,f). Imagines of scaffold seeded with rBMSCs in absence (a,c,e), or presence (b,d,f) of HUVEC on the well bottom. Magn. 4x (a,b) and 10x (c,d,e,f).*

5.3 X-RAY AND MICROCT

X Rays showed a good positioning of the implants, with macroscopic signs of integration in the experimental groups at 4 and 8 weeks of follow up (Fig.15).
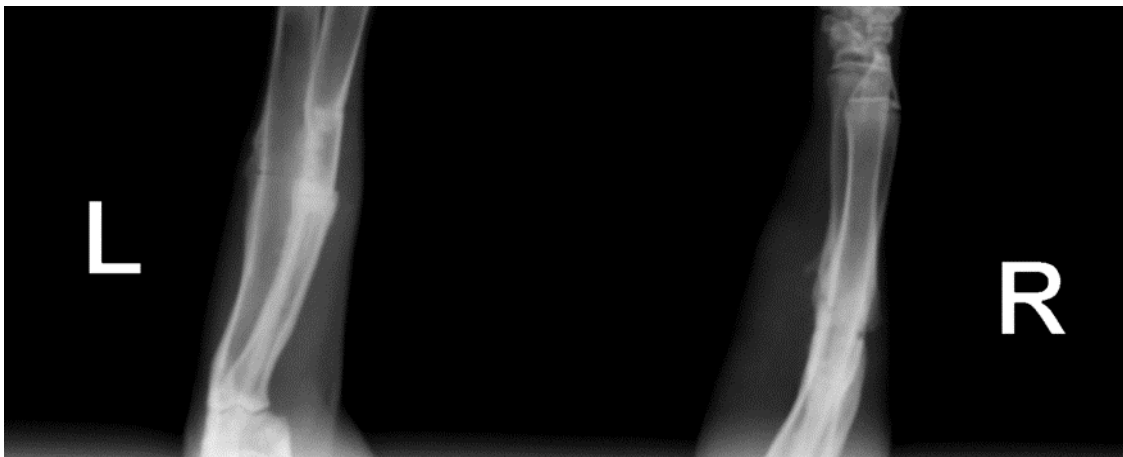

Figure 15 *X rays at the explant time of 8 weeks, experimental group.*

Microtomography analysis (Fig. 16) showed that the main differences were related to the experimental times and to the use of rBMSC. The contribution of the vascular axis deviation within the defect may be highlighted by a greater tendency to bone graft and native cortical bone remodeling activities over time.
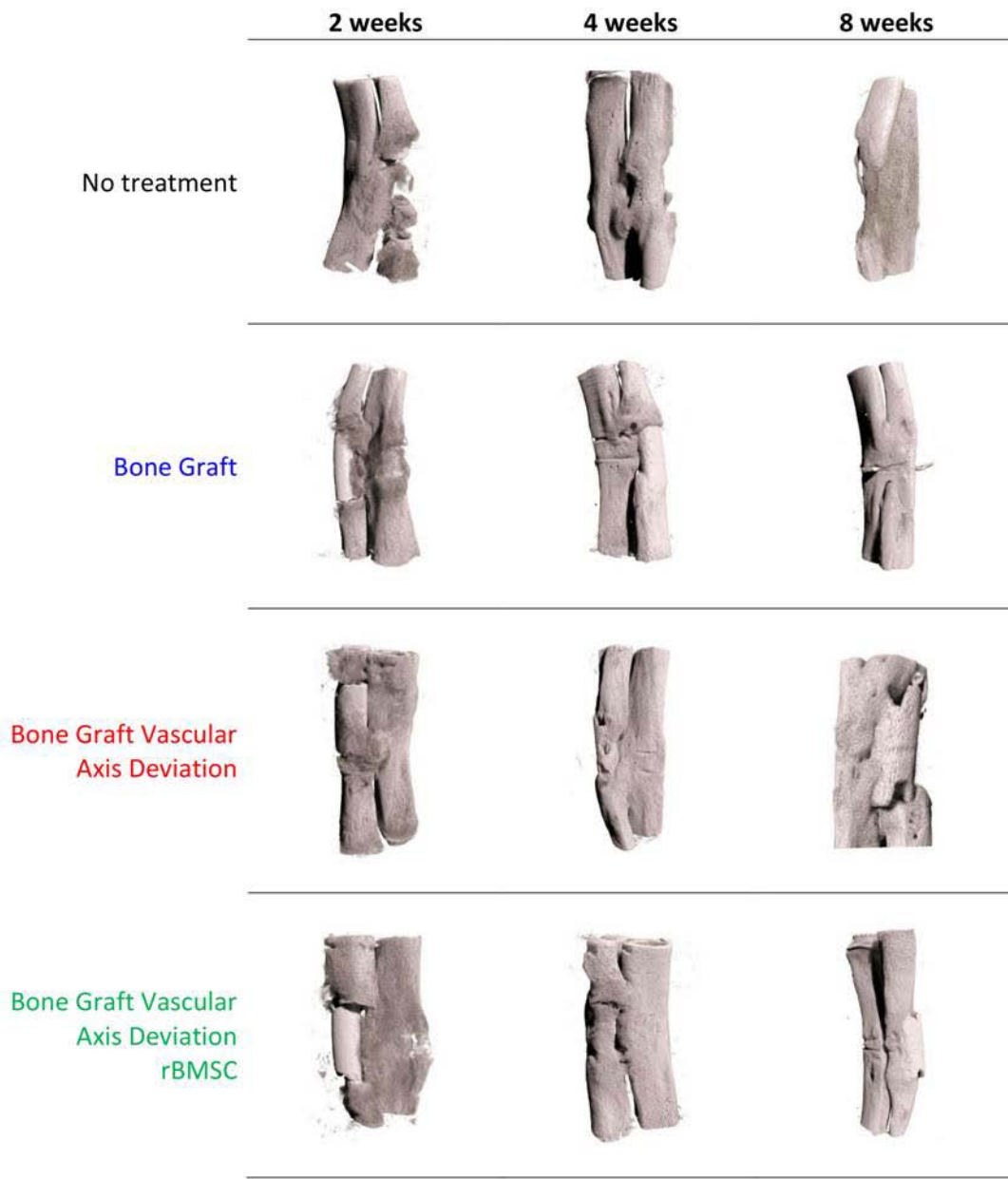
Figure 16 *3D representative models of samples analysed with micro-CT.*

Measured parameters highlighted that Callus density, *Cl.V/TV* was higher in radii treated with bone graft and vascular axis deviation or with bone graft alone in comparison to the other treatments, but in radii treated with bone graft alone *Cl.V/TV* decreased significantly ($p < 0.05$) in comparison to those treated with bone graft and vascular axis deviation (Figure 17a). Callus Index (*Cl.Ind*) decreased significantly ($p < 0.005$) in radii treated with bone graft and vascular axis deviation in comparison to those treated with bone graft at 8 weeks, as well as ($p < 0.005$) in those treated with bone graft with vascular axis deviation and BIOPAD® scaffold seeded with rBMSC in comparison to those treated with bone graft with vascular axis deviation at 4 weeks (Figure 17b). Volumetric Bone/Implant contact (*VBIC*) increased ($p < 0.05$) in radii treated with bone graft with vascular axis deviation in comparison to those treated with bone graft at the longest experimental time (Figure 17c).
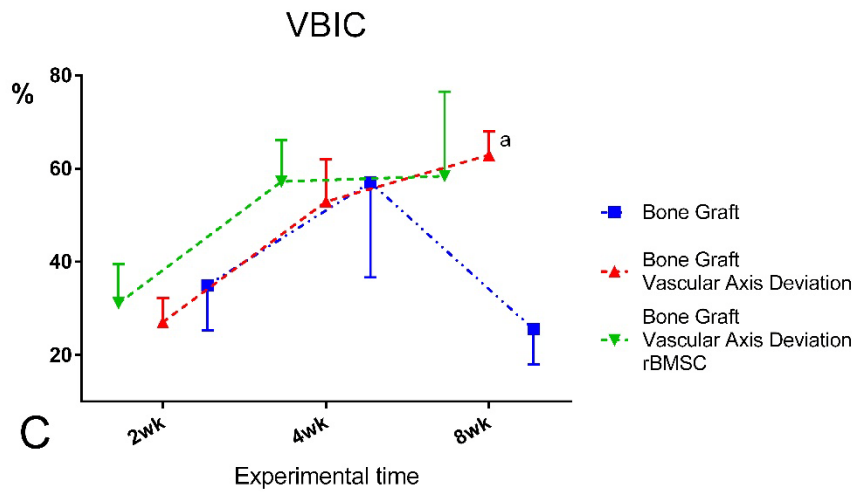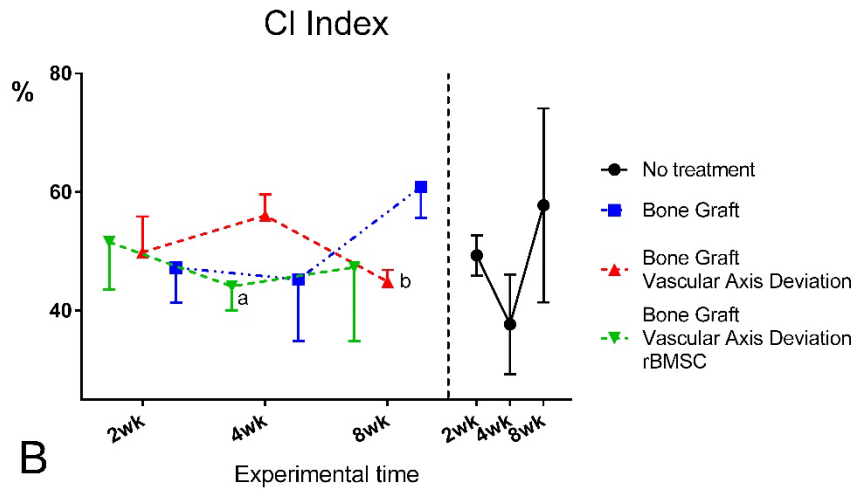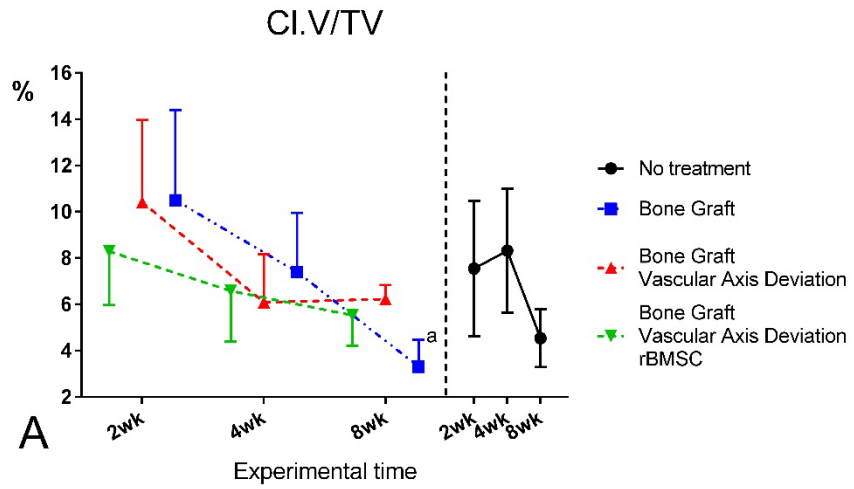
CI.V/TV

A

Legend:
- No treatment (black circle)
- Bone Graft (blue square)
- Bone Graft Vascular Axis Deviation (red triangle)
- Bone Graft Vascular Axis Deviation rBMSC (green triangle)

CI Index

B

Legend:
- No treatment (black circle)
- Bone Graft (blue square)
- Bone Graft Vascular Axis Deviation (red triangle)
- Bone Graft Vascular Axis Deviation rBMSC (green triangle)

VBIC

C

Legend:
- Bone Graft (blue square)
- Bone Graft Vascular Axis Deviation (red triangle)
- Bone Graft Vascular Axis Deviation rBMSC (green triangle)

Figure 17 *Micro-CT quantitative 3D analysis (Mean, BCa 95% CI). A) results relative to Callus density Cl.V/TV: Bone graft and Vascular axis deviation group versus Bone graft group at 8 weeks ([a], p < 0.05); B) results relative to Callus Index Cl.Ind: Bone graft, Vascular axis deviation and BMC group versus Bone graft and Vascular axis deviation group at 4 weeks ([a], p < 0.005) and Bone graft and Vascular axis deviation group versus Bone graft group at 8 weeks ([b], p < 0.005); C) results relative to Volumetric Bone/Implant contact VBIC: Bone graft, Vascular axis deviation and BMC group versus Bone graft and Vascular axis deviation group (a, p < 0.05).*

5.4 HISTOLOGICAL AND IMMUNOHISTOCHEMICAL ANALYSIS OF RADIUS

All animals treated reached the end of the expected experimental time without any clinical complications or evidence of lamness during all experimental time; recovery from surgery was rapid and all animals were able to feed and walk normally in an hour. Macroscopic evaluations did not highlight any evidence of inflammation, infection, hematoma, oedema or reaction in the tissues surrounding the radius.

The native structure and architecture of the bone around the implant appeared preserved, as the adjacent segment of ulna, and the surgical procedure for the insertion of bone graft did not altered the physiological structure of the anatomic region. In some cases, the formation of a synostosis between radio and ulna was noted (Fig. 18).
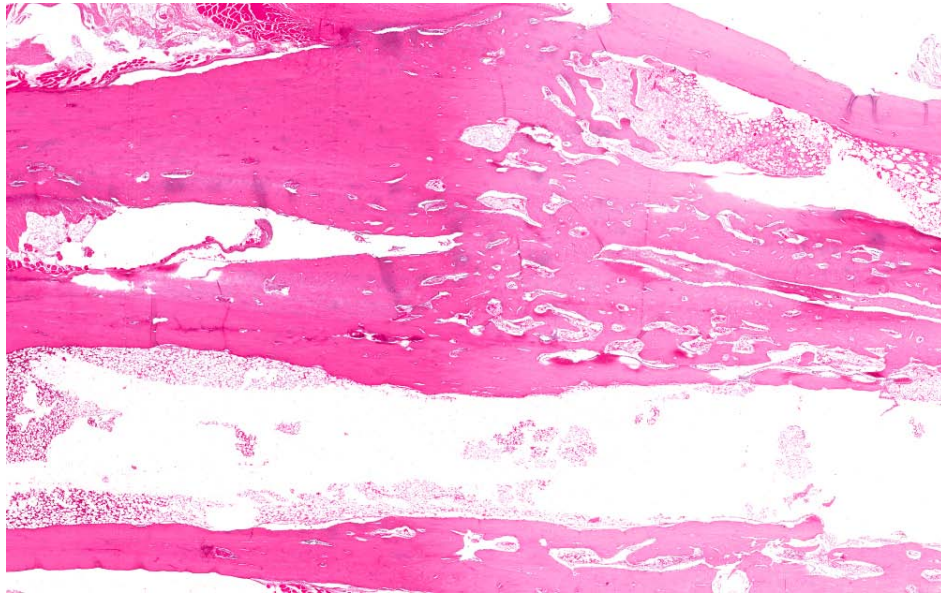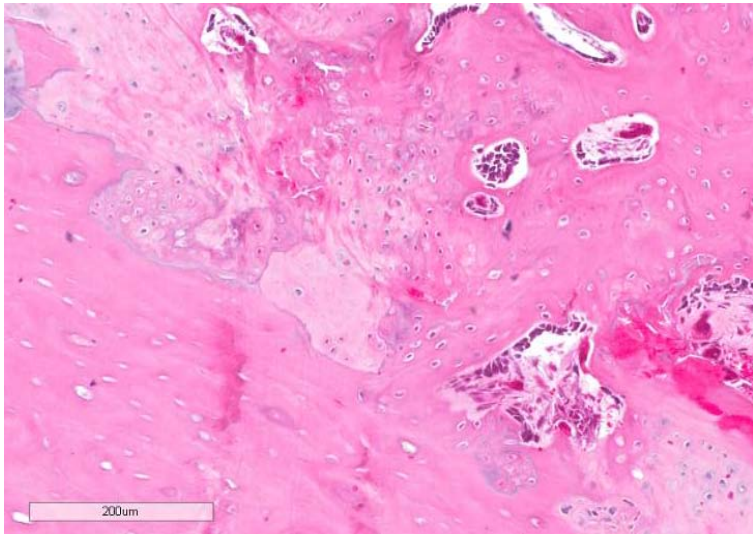
Figure 18   *Presence of synostosis between radio and ulna. Hematoxylin/Eosin staining; 2 x magnification.*
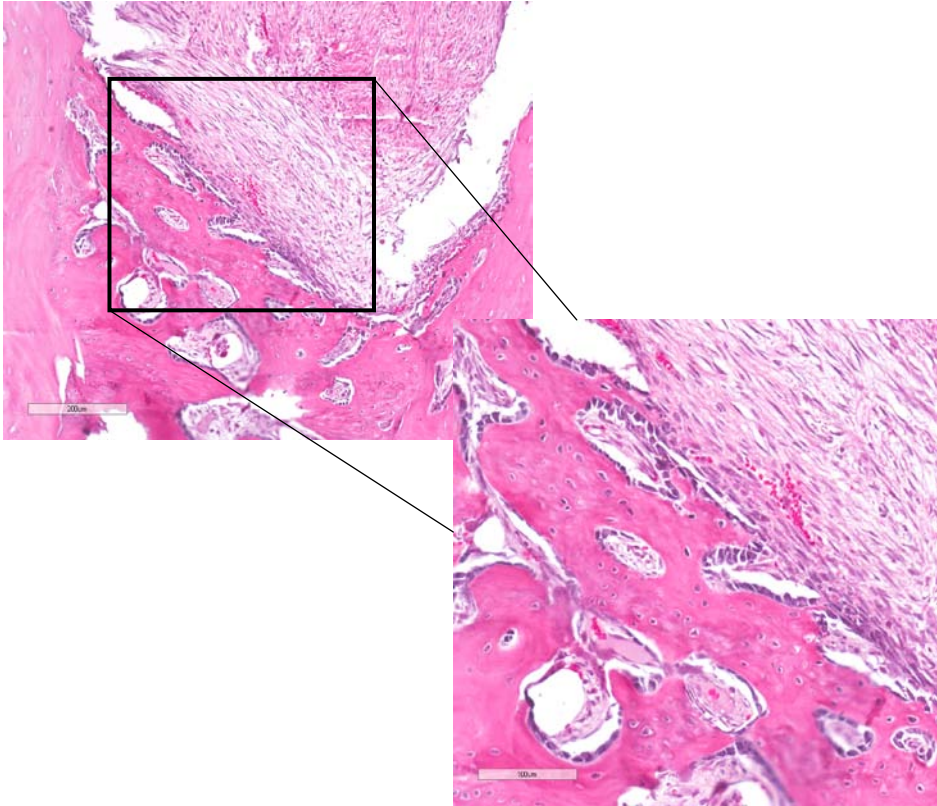
The integration of the graft at both the extremities of the defect appeared still incomplete, the graft was observed generally in place even though not completely aligned in some specimens.

At the longer experimental time (8 weeks), in the samples, which underwent surgery of vascular deviation with and without rBMSC, some contact areas of the graft in continuity with surrounding bone can be observed. In the contact fissure at the interface between graft and bone it can be appreciated the presence of monolayer of osteoblasts on the trabeculae, lacunae filled with osteocytes and vessels (Fig.19).

The onset of phenomenon of endochondral ossification seemed to be present in the areas of incomplete osteointegration, between graft and bone (Fig.20).

a

b

Figure 19 *Detail of integration of graft to bone (a) and layer of osteoblasts on the trabeculae at the interface between bone and graft (b).*
Hematoxylin/Eosin staining; 5x and 10 x magnification.

It can be appreciated the presence of cartilagineous tissue, underlined by the less bright staining, at the interface between bone and graft, proceeding from the innermost extremities of the native bone, with zones of proliferation containing flattened chondrocytes in clusters or oriented in almost a columnar shape, interspersed in the territorial matrix (Fig. 21).
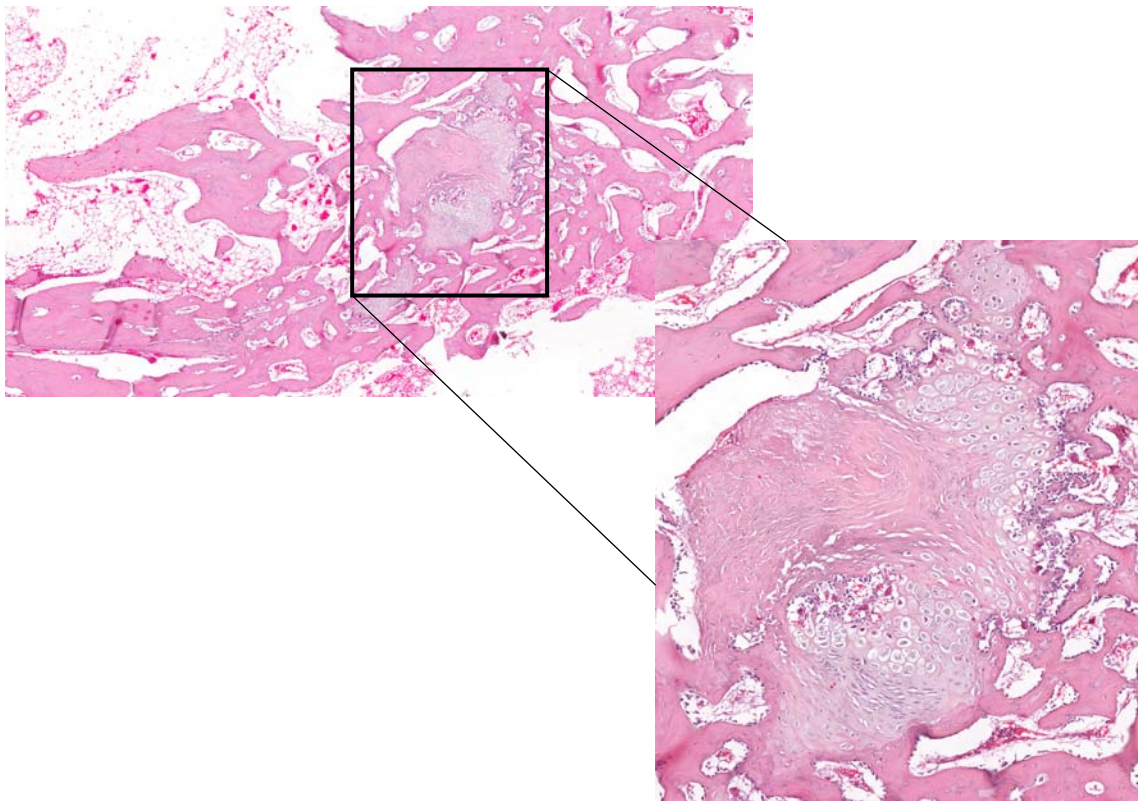

Figure 20 *Endochondral ossification at the interface between bone and graft.*
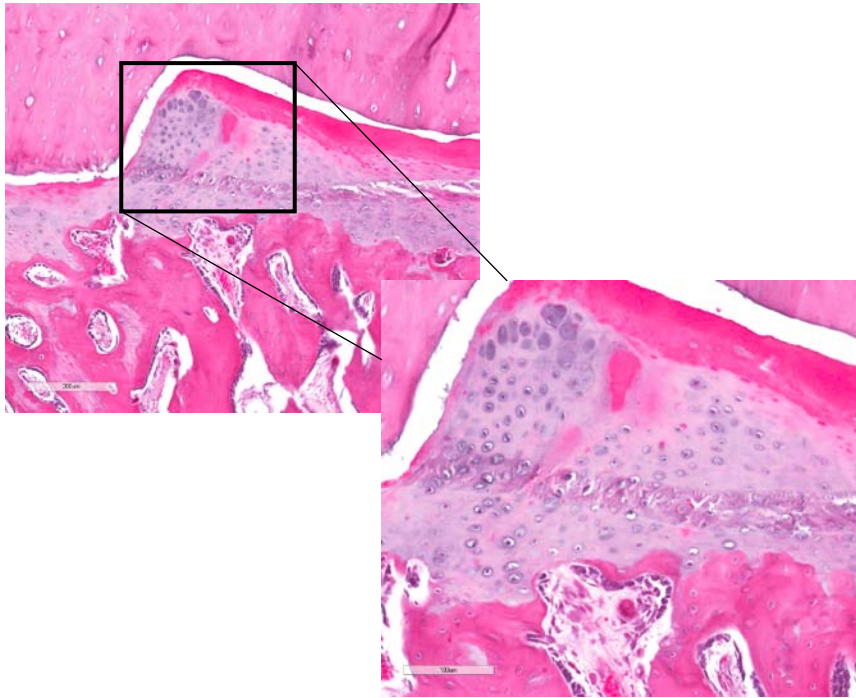*Hematoxylin/Eosin staining; 5x and 10 x magnification.*

Figure 21 *Cartilagineous tissue at the interface between bone and graft, proceeding from the innermost extremities of the native bone, with zones of proliferation containing flattened chondrocytes in clusters or oriented in almost a columnar shape.*
Hematoxylin/Eosin staining; 5x and 10 x magnification.

As far as the groups left untreated or underwent graft alone surgery, two major trends were found: in some cases the bone graft appeared completely not integrated (Fig. 22 a), without any signs of beginning of remodeling, aimed at the integration of the graft with the rest of the segment; in other samples the extremities of the graft appeared merged to form a synostosis, which does not match the normal physiology of the radius (Fig. 22 b).
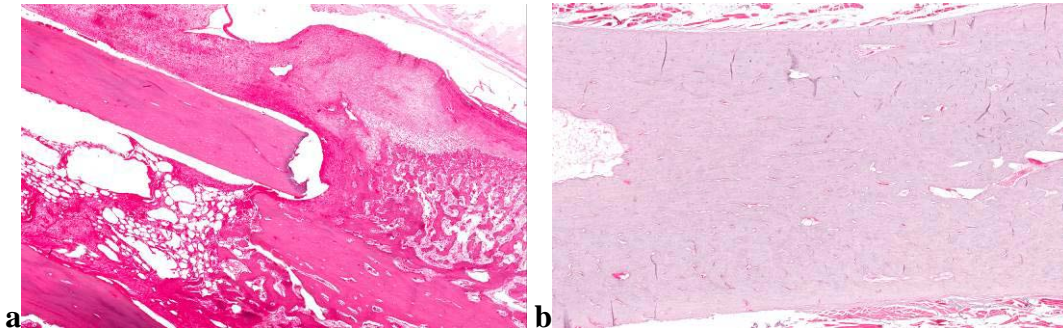
Figure 22   *Failed integration between bone and graft (a) and synostosis between ossification at the interface between the extremities of the graft (b).*
Hematoxylin/Eosin staining;10 x magnification.

Immunohistochemistry qualitative evaluations of VEGF staining showed a greater antibody positivity in the samples treated with the vascular axis deviation, in which was observed in particular the area of interface between bone and graft. The samples that were not subjected to axis deviation showed instead a milder reactivity to VEGF (Figure 23).
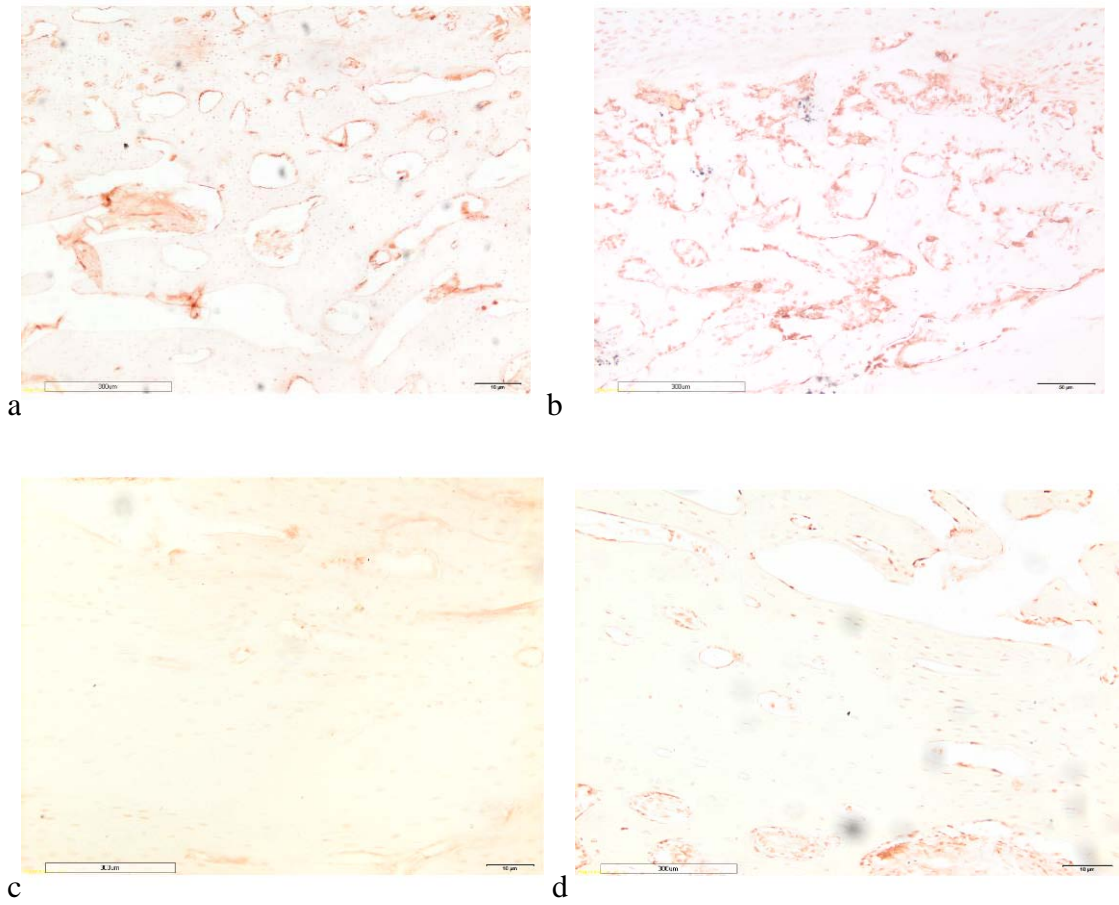
a   b

c   d

Figure 23   *Images of VEGF immunohistochemical staining in vascular deviation axis group (a,b) and control groups (c,d).*

10 x magnification.

CHAPTER 6
DISCUSSION

The repair of long bone defects represents a challenge for the orthopaedic surgeons, with multiple described techniques that offer positive aspects but also carry out strong drawbacks. The allograft substitution is nowadays the most frequently performed surgery in this occurrences, offering the benefits to provide a material which is already perfectly organized in its structure and even without cellular component, it represents an optimal scaffold for the patient to be colonized. The conformation is optimal since the same skeletal districts are used as allograft, and the quantity of tissue to be transplanted is not limited. The potential risk of infective or transmissible diseases is strongly limited by the harvesting/storing protocols and the multiple controls on specimens of explanted tissue. Major drawbacks of this techniques are the limited amount of donors, the high costs for all the process and the ability of the host bone to colonize only one centimeter of the implanted allograft at both edges, resulting in an allograft which is composed only by mineralized tissue. After time, with the mechanical stresses of the regular life, the graft is often affected by small or massive fractures, which has no ability to heal since no osteoblast cellular component is present at its inside. Aim of the current project was to try to implement the graft colonization abilities of the patient. The basis of the idea was that there can be no graft colonization without angiogenesis: new vessels, built by the host in the contest of the implanted tissue, would deliver stem cells, nutritive substances and all the regenerative network useful for the graft colonization. The neoangiogenesis require a main vessel to start from, so the original idea was to make a microsurgical anastomosis with a vessel passing into the cylindrical graft. the small size of the animal model and other technical limitation led us to the idea of inserting a vascular bundle in the graft without cutting and re-suturing it. The median bundle in the rabbit forearm is particularly easy to find and it is close to the radial shaft: it represents an optimal anatomical location in a good animal model for this purpose.

No issues arose in the course of the surgery: the opportunity to avoid the use of microvascular sutures helped in keeping the procedure simple and rapid. The fixation of the raft represented the most demanding step during the procedure: in cases of vascular bundle deviation in the graft the cylinder was not strong enough to be positioned press fit so a secure fixation was required, whether with 2 polysorb stitches or metallic circlages.

At explant times the first main goal of the procedure was achieved: no signs of inflammation, infection, edema, neurovascular deficiency were observed in any animal, so the whole procedure, in all the experimental variants, can be considered safe. All the performed steps were performed in good aseptic condition, the storing protocols were safe, and all the implanted material were not contaminated as well. The integration of the graft with the surrounding bone was more evident with the increasing follow up time, mostly at 8 weeks: this indicates that probably 2 and 4 weeks are not sufficient to see a good graft integration process, and the experimental times should have been prolonged to 12 and 16 weeks. The occasional synostosis formation between ulna and radius can be explained with an excess of regenerative process in a district with a very limited movement activity, since rabbits have no pronosupination and a synostosis between the two forearm bones is sometimes naturally present.

The cell cultures and expansion provided additional essential informations: all the rBMSC are able to differentiate in adipogenic, chondrogenic and osteogenic cell lineages in appropriate environments expressing marker and genes typical of the specific lineage. This indicates that these cells are extremely active with a strong plasticity, a key feature for the experiment. Most important it is the osteogenic capability of these cells, highly indicated by the high expression of genes typical of the differentiation towards this lineage.

The analysis of the cell culture on the collagenic scaffold pointed out that the cells are highly represented in the biomaterial and are distributed in the whole contest of the scaffold itself and not only on the surface, indicating a good tolerability of the collagen scaffold for these type of stem cells. Furthermore, as support of this factor, the

LIVE&DEAD assessment showed that the totality of cells was alive, spread and organized at 24 hours and at 2 weeks after the seeding.

The micro-CT analysis was assessed in order to evaluate the increased remodeling activity of the bone (graft or host) and the efficacy of the vascular deviation. The Callus density was higher in specimens treated with bone graft and vascular axis deviation or with bone graft alone in comparison to the empty controls. In radii treated with bone graft alone the Callus density decreased over time in comparison to those treated with bone graft and vascular axis deviation. This may indicate that in the bone graft alone group there is a higher remodeling of the graft as consequence of the regular biologic processes, while in the second group the callus density decreases slower due to the new bone synthesis promoted by the cellular component provided by the vascular bundle deviation.

The Callus Index decreased significantly in radii treated with bone graft with vascular axis deviation as well as in those treated with bone graft with vascular axis deviation and BIOPAD® scaffold seeded with rBMSC in comparison to those treated with bone graft with vascular axis deviation.

Another important aspect is that the Volumetric Bone/Implant contact significantly increased in radii treated with bone graft with vascular axis deviation in comparison to those treated with bone graft at the longest experimental time: this support the idea that the vascular bundle may provide a supplement of cells with regenerative capabilities.

Histology seemed to confirm the trend observed with microCT results, showing clear signs of ossification and integration of the graft to the surrounding bone, with a high presence of vessels, as indicated also by immunohistochemical analysis. The incomplete integration can be considered so consequence of the short experimental time; in fact, the evidence of endochondral ossification suggests that at longer experimental times a greater osteointegration might be appreciated. In addition, a However, the vascular axis deviation seemed to ha exerted a trophic effect, increasing the presence of vessel and stimulating bone metabolism.

The influence of the biomaterial supplement to this procedure (BIOPAD® scaffold plus concentrated bone marrow cells) is unclear in this evaluation even if associated with a

better outcome: the trophic effects of vascular deviation, in fact, have probably overlapped the influence of material and rBMSCs, making difficult to assess if there was a synergistic effect and to what extent.

CHAPTER 7
CONCLUSIONS

As expected, the obtained results showed that the critical size defect was not completely healed at the described experimental time. Nevertheless, the experimental groups with vascular axis deviation showed a higher neoangiogenic activity and bone turnover, lay the foundation for an active integration of the bone graft. *In vitro* tests suggested that the rBMSC supplement with collagen biomaterial might be effective in terms of repair process stimulation. rBMSC cells showed pluripotent abilities and a proliferation increment in presence of endothelial cells.

As collateral observation, the animal model set up for this study showed to be a good model for critical size defect and critical size defect restoration, with the note that the experimental time should not stop at 8 weeks, but should be continued at least up to 12 weeks. In addition, a more effective stabilization of the graft should be investigated, in order to mimic the clinical post surgical condition, that facilitates the maintenance in place and the integration of the graft.

The future perspective for this study is to be confirmed with longer follow up and possibly in larger animal models (sheep for example) before step up to humans. Another interesting development could be to test different bone substitutes with the same procedure, and to compare them to the healing abilities of the bony allograft. In case of positive results, it would be extremely positive to combine the pros of a bone substitute, which eliminates the cons of allografting, with a vascular procedure, which eliminates the major cons of the bony substitute like the non osteointegration and substitution.

REFERENCES

1. Blumenfeld, S. Srouji, Y. Lanir, D. Laufer, E. Livne. Enhancement of bone defect healing in old rats by TGF-β and IGF-1 Exp Gerontol, 37 (2002), pp. 553–565.

2. Perry C.R. Bone repair techniques, bone graft, and bone graft substitutes. Clin Orthop Relat Res, 360 (1999), pp. 71–86.

3. J.R. Clements, B.B. Carpenter, J.K. Pourciau. Treating segmental bone defects: a new technique. J Foot Ankle Surg, 47 (2008), pp. 350–356.

4. Rimondini L, Nicoli-Aldini N, Fini M, et al. In vivo experimental study on bone regeneration in critical bone defects using an injectable biodegradable PLA/PGA copolymer. Oral Surg Oral Med Oral Pathol Oral Radiol Endod. 2005 Feb;99(2):148-54.

5. Einhorn TA. Clinically applied models of bone regeneration in tissue engineering research. Clin Orthop Relat Res. 1999 Oct;(367 Suppl):S59-67.

6. Lindsey RW, Gugala Z, Milne E, et al. The efficacy of cylindrical titanium mesh cage for the reconstruction of a critical-size canine segmental femoral diaphyseal defect. J Orthop Res. 2006 Jul;24(7):1438-53.

7. Williams D.F.. On the nature of biomaterials. Biomaterials, 30 (2009), pp. 5897–5909.

8. Kokubo S, Fujimoto R, Yokota S, et al. Bone regeneration by recombinant human bone morphogenetic protein-2 and a novel biodegradable carrier in a rabbit ulnar defect model Biomaterials, 24 (2003), pp. 1643–1651.

9. Han S.-O, Mahato RI, Sung YK, Kim SW. Development of biomaterials for gene therapy. Mol Ther, 2 (2000), pp. 302–317.

10. Hubbell JA. Biomaterials in tissue engineering. Nat Biotechnol, 13 (1995), pp. 565–576.

11. Richards RG. AO Research Institute Davos within the AO Foundation: a model for translation of science to the clinics. J Orthop Transl, 1 (2013), pp. 11–18.

12. Liu G, Zhao L, Zhang W et al. Repair of goat tibial defects with bone marrow stromal cells and beta-tricalcium phosphate. J Mater Sci Mater Med. 2008 Jun;19(6):2367-76. Epub 2007 Dec 25.

13. Romana MC and Masquelet AC. Vascularized periosteum associated with cancellous bone graft: an experimental study. Plastic and Reconstructive Surgery 1990; 85 (4): 587-592.

14. Cierny G 3rd, Zorn KE. Segmental tibial defects. Comparing conventional and Ilizarov methodologies. Clin Orthop Relat Res. 1994 Apr;(301):118-23.

15. Committee on Patient Safety/Committee on Biological Implants Tissue Work Group: Musculoskeletal allograft tissue safety. Presented at: The Annual Meeting of the American Academy of Orthopaedic Surgeons; February 22-28, 2003; New Orleans, LA.

16. Dion N, Sim FH. The use of allografts in musculoskeletal oncology. Instr Course Lect 51:499, 2002.

17. Mnaymneh W, Malinin T: Massive allografts in surgery of bone tumors. Orthop Clin North Am 20:3, 1989

18. Mnaymneh W, Malinin TI, Lackman RD, Hornicek FJ, Ghandur L: Massive distal femoral osteoarticular allografts following resection of bone tumors. Clin Orthop 303:103, 1994.

19. Boyce T, Edwards J, Scarborough: Allograft bone: the influence of processing on safety and performance. Orthop Clin North Am 30:4, 1999.

20. Lavernia CJ1, Malinin TI, Temple HT, Moreyra CE. Bone and tissue allograft use by orthopaedic surgeons. J Arthroplasty. 2004 Jun;19(4):430-5.

21. Chapman MW, Bucholz R, Cornell C. Treatment of acute fractures with a collagen-calcium phosphate graft material. A randomized clinical trial. J Bone Jt Surg Am, 79 (1997), pp. 495–502.

22. Muscolo D.L, Ayerza MA, La A.-T. Massive allograft use in orthopedic oncology. Orthop Clin North Am, 37 (2006), pp. 65–74.

23. Gazdag AR, Lane JM, Glaser D, Forster RA. Alternatives to autogenous bone graft: efficacy and indications. J Am Acad Orthop Surg, 3 (1995), pp. 1–8.

24. Oest MEDK, Kong HJ, Mooney DJ, Guldberg RE. Quantitative assessment of scaffold and growth factor-mediated repair of critically sized bone defects. J Orthop Res, 25 (2007), pp. 941–950.

25. Giannini S, Buda R, Vannini F, Cavallo M, Grigolo B. One-step bone marrow-derived cell transplantation in talar osteochondral lesions. Clin Orthop Relat Res. 2009 Dec;467(12):3307-20.

26. Vannini F, Battaglia M, Buda R, et al. "One step" treatment of juvenile osteochondritis dissecans in the knee: clinical results and T2 mapping characterization. Orthop Clin North Am. 2012;43:237–44.

27. Giannini S, Buda R, Cavallo M, et al. Cartilage repair evolution in post-traumatic osteochondral lesions of the talus: from open field autologous chondrocyte to bone-marrow-derived cells transplantation. Injury. 2010;41:1196–1203.

28. Caplan AI. Adult mesenchymal stem cells for tissue engineering versus regenerative medicine. J Cell Physiol. 2007;213:341–347.

29. Dominici M, Pritchard C, Garlits JE, Hofmann TJ, Persons DA, Horwitz EM. Hematopoietic cells and osteoblasts are derived from a common marrow progenitor after bone marrow transplantation. PNAS. 2004;101:11761–11766.

30. Galois L, Freyria AM, Herbage D, Mainard D. Cartilage tissue engineering: state-of-the-art and future approaches. Pathol Biol Paris. 2005;53:590–598.

31. Mazzucco L, Medici D, Serra M, Panizza R, Rivara G, Orecchia S, Libener R, Cattana E, Levis A, Betta PG, Borzini P. The use of autologous platelet gel to treat difficult-to-heal wounds: a pilot study. Transfusion. 2004;44:1013–1018.

32. Olmsted-Davis EA, Gugala Z, Camargo F, Gannon FH, Jackson K, Kienstra KA, Shine HD, Lindsey RW, Hirschi KK, Goodell MA, Brenner MK, Davis AR. Primitive adult hematopoietic stem cells can function as osteoblast precursors. PNAS. 2003;100:15877–15882.

33. Oreffo RO, Cooper C, Mason C, Clements M. Mesenchymal stem cells: lineage, plasticity, and skeletal therapeutic potential. Stem Cell Rev. 2005;1:169–178

34. Clarke B. Normal Bone Anatomy and Physiology. Clin J Am Soc Nephrol. 2008 Nov; 3(Suppl 3): S131–S139.

35. Eriksen EF, Axelrod DW, Melsen F. Bone Histomorphometry, New York, Raven Press,1994, pp1 –12.

36. Hall BK, Miyake T. All for one and one for all: condensations and the initiation of skeletal development. Bioessays 2000;22:138–47.

37. Kanczler J.M., Oreffo R.O.C. Osteogenesis and angiogenesis: the potential for engineering bone. European Cells and Materials Vol. 15 2008 (pages 100 - 114)

38. Zelzer E, McLean W, Ng YS, et al. (2002) Skeletal defects in VEGF(120/120) mice reveal multiple roles for VEGF in skeletogenesis. Development 129: 1893-1904.

39. Street J, Bao M, deGuzman L, et al. Vascular endothelial growth factor stimulates bone repair by promoting angiogenesis and bone turnover. Proc Natl Acad Sci USA (2002) 99: 9656-9661.

40. Gerber HP, Ferrara N Angiogenesis and bone growth. Trends Cardiovasc Med (2000) 10: 223-228.

41. Sfeir, C.; Ho, L.; Doll, BAet al. Fracture repair. In: Lieberman, JR.; Friedlaender, GE., editors. Bone regeneration and repair. Humana Press; Totowa, NJ: 2005. p. 21-44.

42. Gerstenfeld LC, Alkhiary YM, Krall EA, et al. Three-dimensional reconstruction of fracture callus morphogenesis. Journal of Histochemistry & Cytochemistry. 2006; 54(11):1215–28.

43. Marsell R, Einhorn T.A. The biology of fracture healing. Injury. 2011 June; 42(6): 551–555.

44. Giordano A, Galderisi U, Marino IR. From the laboratory bench to the patient's bedside: an update on clinical trials with mesenchymal stem cells. J Cell Physiol 2007; 211: 27-35.

45. Tzioupis CC, Giannoudis PV. The Safety and Efficacy of Parathyroid Hormone (PTH) as a Biological Response Modifier for the Enhancement of Bone Regeneration. Curr Drug Saf 2006; 1: 189-203.

46. Carofino BC, Lieberman JR. Gene therapy applications for fracture-healing. J Bone Joint Surg Am 2008; 90 Suppl 1: 99-110.

47. Fröhlich M. Childs SG. Stimulators of bone healing. Biologic and biomechanical. Orthop Nurs 2003; 22: 421-428.

48. Carano RAD, Filvaroff EH. Angiogenesis and bone repair. Drug Discov Today 2003;8:980–9.

49. Huang YC, Kaigler D, Rice KG, Krebsbach PH, Mooney DJ. Combined angiogenic and osteogenic factor delivery enhances bone marrow stromal cell-driven bone regeneration. J Bone Miner Res 2005; 20:848–57

50. Zuk PA, Zhu M, Mizuno H et al. Multilineage cells from human adipose tissue: implications for cell-based therapies. Tissue Eng. 2001 Apr;7(2):211-28.

ACKNOWLEDGMENTS